AUDRIUS MERFELDAS

DEVELOPMENT AND INVESTIGATION OF NEAR-FIELD RADIATED SUSCEPTIBILITY MAPPING METHODOLOGY FOR RADIO FREQUENCY DEVICES

SUMMARY OF DOCTORAL DISSERTATION

TECHNOLOGICAL SCIENCES, ELECTRICAL AND ELECTRONICS ENGINEERING (T 001)

Kaunas
2021

KAUNAS UNIVERSITY OF TECHNOLOGY

AUDRIUS MERFELDAS

DEVELOPMENT AND INVESTIGATION OF NEAR-FIELD RADIATED SUSCEPTIBILITY MAPPING METHODOLOGY FOR RADIO FREQUENCY DEVICES

Summary of Doctoral Dissertation
Technological Sciences, Electrical and Electronics Engineering (T 001)

2021, Kaunas

The doctoral dissertation was prepared at Kaunas University of Technology, Faculty of Electrical and Electronics Engineering, Department of Electronics Engineering, in 2016–2020.

Scientific supervisor:
Prof. Dr. Darius GAILIUS (Kaunas University of Technology, Technological Sciences, Electrical and Electronics Engineering, T 001).

Editor: Brigita Brasienė (Publishing house "Technologija")

Dissertation Defence Board of Electrical and Electronics Engineering Science Field:
Prof. Dr. Liudas MAŽEIKA (Kaunas University of Technology, Technological Sciences, Electrical and Electronic Engineering, T 001) **– chairman**;
Prof. Dr. Elena JASIŪNIENĖ (Kaunas University of Technology, Technological Sciences, Electrical and Electronic Engineering, T 001);
Prof. Dr. Wlodek J. KULESZA (Blekinge Institute of Technology, Sweden, Technological Sciences, Electrical and Electronic Engineering, T 001);
Prof. Dr. Jurij NOVICKIJ (Vilnius Gediminas Technical University, Technological Sciences, Electrical and Electronic Engineering, T 001);
Prof. Dr. Darius VIRŽONIS (Kaunas University of Technology, Technological Sciences, Electrical and Electronic Engineering, T 001).

The official defence of the dissertation will be held at 10 a.m. on 24th of May, 2021 at the public meeting of the Dissertation Defence Board of Electrical and Electronics Engineering Science Field in Dissertation Defence Hall at Kaunas University of Technology.

Address: K. Donelaičio Str. 73-403, 44249 Kaunas, Lithuania.
Tel. no. (+370) 37 300 042; fax. (+370) 37 324 144; e-mail doktorantura@ktu.lt.

The summary of dissertation was sent on 23th of April, 2021.
The doctoral dissertation is available on the internet http://ktu.edu and at the library of Kaunas University of Technology (K. Donelaičio St. 20, 44239 Kaunas, Lithuania).

KAUNO TECHNOLOGIJOS UNIVERSITETAS

AUDRIUS MERFELDAS

ELEKTRONINĖS AUKŠTADAŽNĖS ĮRANGOS ATSPARUMO SPINDULIUOJAMIEMS ELEKTROMAGNETINIAMS TRIKDŽIAMS TYRIMAS ARTIMAME LAUKE (METODIKOS SUKŪRIMAS IR TAIKYMAS)

Daktaro disertacijos santrauka
Technologijos mokslai, elektros ir elektronikos inžinerija (T 001)

2021, Kaunas

Disertacija rengta 2016–2020 metais Kauno technologijos universiteto Elektros ir elektronikos fakultete Elektronikos inžinerijos katedroje.

Mokslinis vadovas:
Prof. Dr. Darius GAILIUS (Kauno technologijos universitetas, technologijos mokslai, elektros ir elektronikos inžinerija, T 001).

Lietuvių kalbos redaktorė:
Violeta Meiliūnaitė (Leidykla „Technologija“).

Elektros ir elektronikos inžinerijos mokslo krypties disertacijos gynimo taryba:
Prof. dr. Liudas MAŽEIKA (Kauno technologijos universitetas, technologijos mokslai, elektros ir elektronikos inžinerija, T 001) **– pirmininkas**;
Prof. dr. Elena JASIŪNIENĖ (Kauno technologijos universitetas, technologijos mokslai, elektros ir elektronikos inžinerija, T 001);
Prof. dr. Wlodek J. KULESZA (Blekingo Technologijos institutas, Švedija, technologijos mokslai, elektros ir elektronikos inžinerija, T 001);
Prof. dr. Jurij NOVICKIJ (Vilniaus Gedimino Technologijos Universitetas, technologijos mokslai, elektros ir elektronikos inžinerija, T 001);
Prof. dr. Darius VIRŽONIS (Kauno technologijos universitetas, technologijos mokslai, elektros ir elektronikos inžinerija, T 001).

Disertacija bus ginama viešame Elektros ir Elektronikos mokslo krypties disertacijos gynimo tarybos posėdyje, 2021 m. gegužės 24 d. 10 val. Kauno technologijos universiteto Disertacijų gynimo salėje.

Address: K. Donelaičio g. 73-403, 44249 Kaunas, Lietuva.
Tel. (+370) 37 300 042; faks. (+370) 37 324 144; el. paštas doktorantura@ktu.lt.

Disertacijos santrauka išsiųsta 2021 balandžio 23.
Su disertacija galima susipažinti internetinėje svetainėje http://ktu.edu ir Kauno technologijos universiteto bibliotekoje (K. Donelaičio g. 20, 44239 Kaunas).

LIST OF ABBREVIATIONS

AC – Alternating Current
BCI – Bulk Current Injection Method
CATV – Cable Television
DUT – Device Under Test
EMC – Electromagnetic Compatibility
FEM – Finite Element Method
GTEM – Gigahertz Transverse Electromagnetic
IC – Integrated Circuit
IoT – Internet of Things
MLCC – Multilayer Ceramic Capacitor
OATS – Open Area Test Site
OLC – Optical Level Control
PCB – Printed Circuit Board
RF – Radio Frequency
SMD – Surface Mount Device
TEM – Transverse Electromagnetic
UP – Uniform Plane
VCO – Voltage Controllable Oscillators
VNA – Vector Network Analyzer
WTEM – Wire Transverse Electromagnetic Cell

INTRODUCTION

Relevance of the work

Successful design and certification processes of modern electronics equipment and systems are closely related to the electromagnetic compatibility and RF pollution evaluation. Upcoming services such as Internet of Things (IoT), 5G, and other modern wireless services are aiming for signal density increase [1] and causing new challenges for radio frequency (RF) devices' technical solutions. New methods for radiated susceptibility mapping and analysis of electronics and high frequency devices would lead to simplified electromagnetic compatibility (EMC) troubleshooting and reducing design challenges. This is very important for medical, automotive, military, aviation, and other applications.

During everyday operations, an electronic device could be exposed to various electromagnetic fields radiated from other devices all around. However, PCB layout issues could lead to serious radiated immunity problems leading to failing of certification. IEC 61000-6-1, IEC 61000-6-2 standards cover the main concepts, frequency ranges, and field strength levels for residential and industrial environments, radiated emissions regulated by IEC 61000-6-3 and IEC 61000-6-4 standards. Both emissions limited above 30 MHz and RF susceptibility starting at 80 MHz are required for any equipment [2]. The end of the frequency range is determined by product standard and applications.

EMC requirements for alternating current (AC) powered equipment are determined by additional standards. The conducted emissions and immunity tests cover 150 kHz – 30 MHz (80 MHz) (IEC 61000-4-6) frequency range. Other measurements and limits for power harmonics (IEC 61000-3-2, IEC 61000-3-12) and flicker (IEC 61000-3-3, IEC 61000-3-11) might be applied for higher power equipment. Various events such as voltage dips, short interruptions and voltage variations (IEC 61000-4-11), surges (IEC 61000-4-5), electrical fast transient (IEC 61000-4-4) and immunity to harmonics and interharmonics (IEC 61000-4-13), and AC magnetic field (IEC 61000-4-8) might be simulated to ensure immunity to power line events. For electronic device quality and reliability, EMC standards require immunity to electrostatic discharge (IEC 61000-4-2).

There are many methods that have been developed for radiated susceptibility testing, while the most popular is anechoic chamber. This method is precise, reliable and ensures good repeatability. However, the price for laboratory equipment is extremely high: high power RF amplifiers, costly RF absorbers and ferrite tiles all over the shielded room, and high power antennas capable to generate standard determined field strength over 10 m or 3 m distance. Though this method qualifies by high repeatability, the informativeness of test results is limited to "Yes/No" type of answers for various frequencies.

Worldwide scientific researches show high interest in near-field probes that might be a useful tool for hotspot localization and troubleshooting. The products that are available on market are concentrated on emissions measurements. Near-field probes utilization for radiated immunity has not been deeply analyzed, providing space for investigation. Scientific researches and personal author experience in EMC testing and RF product design confirm that the instruments in the market are not optimized for a specific frequency range and are mainly focused only on preliminary inspection of radiated emissions. Near-field probe characteristics might be influenced by the persistence of PCB and electronics components leading to varying complicated hotspot localization or wrong solutions, especially for high integrity PCBs.

This indicated a scientific and engineering demand to develop radiated susceptibility investigation methodology and instruments based on near-field probes. The modern modelling software enables possibilities for near-field probe construction optimization for a specific frequency range, PCB component types, and orientation. The author assumes that in order to ensure proper radiated susceptibility mapping for modern high integrity electronic device PCBs, it is important to reach for high spatial resolution near-field probe characterization and investigation of electronic components and PCB persistence influence for system measurements.

Aim and objectives of the work

The main **aim** of this work is the development and analysis of near-field high resolution mapping methodology and instrumentation for radiated susceptibility evaluation of radio frequency equipment.

In order to achieve the aim of this research, the following **objectives** were set:

1. Analysis and comparison of radiated susceptibility testing methods;
2. Development of high resolution magnetic near-field probe and analysis of its magnetic field strength in frequency, spatial and resolution domain in 80–3000 MHz frequency range;
3. Analysis of electronics components persistence for probe magnetic field characteristics;
4. Development of methodology for radiated susceptibility mapping time minimization;
5. Verification of developed methodology by electromagnetic field susceptible radio frequency device printed circuit boards' hotspots localization.

Scientific novelty of the work

1. Novel radiated susceptibility near-field mapping methodology has been developed and investigated for susceptibility hotspots localization of radio frequency printed circuit boards in 80–3000 MHz frequency range.
2. Improved spatial resolution near-field probe has been designed and optimized for adaptive scanning height system in the range of 1–15 mm.
3. Developed detailed common electronic components models for near-field magnetic probe radiation pattern distortion evaluation.
4. Scanning method for faster pre-scan time, allowing average 31% efficiency improvement.

Practical value of the work

Radiated susceptibility near-field mapping methodology has been developed and verified; improved magnetic near-field probe has been designed and optimized for frequency range of 80–3000 MHz and scan heights of 1–15 mm for adaptive scanning systems. Fast pre-scan method has been developed based on -6 dB field aperture for minimizing pre-scan time. Susceptibility hotspots map might contribute for the EMC troubleshooting and provide detailed information on the problematic areas for EMC laboratories and design engineers.

Research methods

A detailed analysis of electromagnetic radio frequency susceptibility testing methods has been done, and near-field scanning technique was chosen for the methodology development. Various constructions of magnetic and electric field probes were analyzed, and CST Studio Suite FEM software was used for the development of improved spatial resolution near-field magnetic probe construction. Utilizing mathematical model, the measurement probes and field monitors the optimization of testing methodology, and the system has been done in the frequency range of 80–3000 MHz. De-embedding of manufactured RF PCB parameters for system calibration was performed in AWR Microwave Office software.

Both developed near-field radiated susceptibility system control and susceptibility map post-processing have been done using Matlab software. The developed methodology was verified using simplified and commercial radio frequency equipment printed circuit boards, and hotspots maps were rendered. The verification has been carried out in gigahertz transverse electromagnetic (GTEM) cell for far-field and near-field susceptibility maps comparison.

Statements presented for defense

1. The near-field radiated susceptibility mapping methodology allows hotspot localization for radio frequency equipment printed circuit boards.

2. Developed magnetic near-field probe improves radiated susceptibility mapping resolution for 80–3000 MHz frequency range.
3. Developed advanced pre-scan method utilizing -6 dB magnetic field aperture minimizes the time of radiated susceptibility mapping.
4. Proximity of electronic surface mount components influences the boundaries of -6 dB magnetic field aperture of proposed near-field probe.

Structure of the dissertation

Dissertation consists of an introduction, 4 chapters, conclusions, list of references, appendixes. The size of the dissertation is 186 pages (and 2 pages of appendixes), 18 tables, 28 equations, 166 figures, 105 references of bibliographic sources.

Approbation of the work

The main scientific results have been published in five articles: two publications in journals, which are indexed in Thomson Reuters List, three in international conference proceedings.

The research results were presented at three international conferences in Lithuania, The Czech Republic, and Italy.

1. RADIATED IMMUNITY METHODS AND ENVIRONMENTS

Many methods have been developed for radiated RF susceptibility testing. Some of them mimic the real impact of radiated interferences, other require less RF (Radio Frequency) power and cheaper equipment or are able to create very high field strength.

Open Area Test Site (OATS) and anechoic chamber are similar methods, where the device under test (DUT) is placed on 0.8 m non-conductive table over large ground plane, according to IEC 61000-4-3 standard. Depending on the frequency range and product standards, radiating antenna is placed 10 m, 3 m, or 1 m distance from DUT for testing in the far field conditions. In order to ensure full exposure of the whole product, DUT is rotated, antenna polarization switched, and the field uniformity in testing area pre-checked. For field uniformity evaluation, uniform plane (UP) is divided into 16 points, and the electric field strength is measured for the whole frequency range (Fig. 1.1). Field uniformity is considered to be appropriate in the case when 75% of tested spatial points field strength fits in $\leq$6 dB [2].

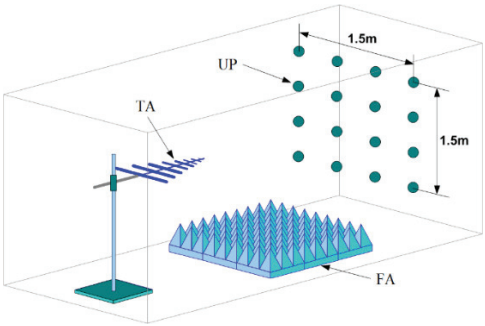

Fig. 1.1. Radiated susceptibility measurement in OATS method setup, where TA – transmitting antenna, UP – uniform field plane, FA – floor absorbers

Nowadays, OATS method is still considerable for pre-compliance testing due to cheaper testing price. However, testing results are sensitive to hardly controllable humidity in the testing site air. Anechoic chamber is a standard and most popular environment for RF susceptibility testing, even though it requires very high cost for RF absorbers and chamber size. Large distance between antenna and DUT requires high RF power, which increases the power handling requirements for RF power amplifier and antenna.

In order to overcome the cons of the mentioned anechoic chamber, the method stripline and TEM (transverse electromagnetic mode) cell methods have been established. The methodology utilizes waveguide and transmission line theories that state similar to free space conditions inside transmission lines, as TEM mode propagation is achieved [3]. Strip line is used mainly for automotive tests according to ISO 11452-5; 150 mm testing volume height allows to use small size equipment (recommended less than 30% of strip line height) [4]. Long testing volume is suitable for the EM field generation for 1.5 m automotive DUT cables.

For larger DUTs, 3 element structures such as TEM cells are required. TEM cell utilizes the advantage of reducing signal plate, called septum, width by adding ground coupling plane at the top of stripline [5]. Having partially shielded environment, only side walls needed to keep fields inside the enclosed and full shielding for radiated emission measurements. Thought TEM cells require much lower RF power for a standard field strength generation, rectangular septum shape have resonances depending on the shape size. The improved version of TEM cell is called GTEM (Gigahertz TEM). For achieving non resonant structure, septum shape designed tapered shape. For keeping the impedance shape of the whole GTEM, the cell is pyramid like. The septum is loaded with distributed 50 Ω load, while all reflections and parasitic fields are absorbed by RF absorbers at the bottom of the cell. Improved wire TEM (WTEM) structure reduces the coupling between septum and DUT, allowing bigger DUT sizes for

testing, while EUROTEM cell adds possibility to shift the electric field orientation with the help of two septum pairs.

Bulk Current Injection method (BCI) was developed by injecting parasitic currents into DUT wires, mainly for automotive equipment [6], but some researches have been done up to 1 GHz [7]. BCI method utilizes current probes placed around the wires and inductive coupling principle. The main disadvantage of radiated susceptibility is that the coupling is indirect.

The reverberation chamber that is opposite to anechoic utilizes the reflections from the conductive walls [8]. This allows very high field strength generation in the internal volume. Superposition of reflections might create peaks and valleys in the EM field. By adding few mode stirrers with moving reflectors, it is possible to create a uniform field. The reverberation chambers are mainly used for automotive, space and aviation radiated susceptibility testing due to big dimensions of DUT.

All radiated susceptibility methods provide only "Pass/Fail" type results that lack more information that is necessary for the PCB troubleshooting. High integrated product PCB layouts might be hard to analyze due to the complexity of schematics. Near-field RF susceptibility mapping could provide detailed information and hotspot localization for these cases. The probe location changes in scanning manner, and different areas of the PCB are analyzed. At small distances from PCB, RF radiation is in near-field where two types of radiation are possible, i.e., electric field and magnetic field radiation. The electric field probe is omnidirectional [9], while magnetic field has directivity [10]. The characteristic of magnetic field to penetrate into deeper PCB layers was the key factor for choosing it for developing near-field radiated susceptibility mapping system.

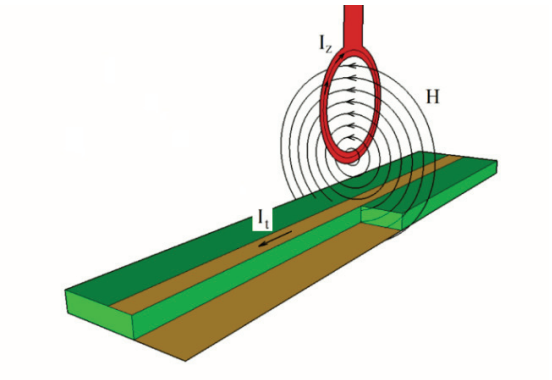

Fig. 1.2. Magnetic near-field probe principle of operation for radiated susceptibility testing

Magnetic near-field probe operation for RF susceptibility test is explained in Fig. 1.2, where RF current fed to probe is creating I_z current flowing in a loop around PCB cutout, resulting in H field. The field penetrating gap between signal and ground conductors of DUT PCB microstrip line develops the signal level at its output.

2. MAGNETIC NEAR-FIELD PROBE

In this research, the magnetic near-field probe has been optimized in 80–3000 MHz frequency range, and the magnetic field focusing was improved by utilizing novel structure. The probe has been developed on l = 15 mm length and w = 8 mm width FR-4 substrate in 1 mm thickness. The probe was encapsulated by r = 4 mm internal radius copper pipe. The PCB trace loop was shaped into square with 4.8 mm edge size from 0.3 mm width microstrip line as presented in Figure 2.1.

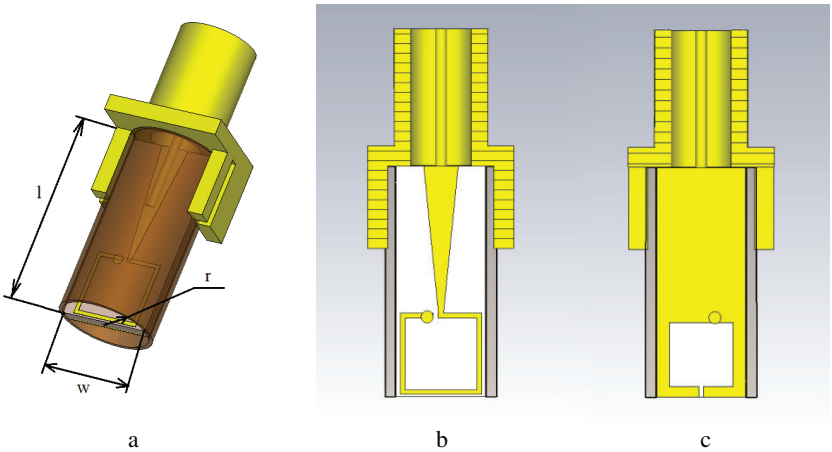

Fig. 2.1. Improved magnetic field probe structure (a) optimized for 80–3000 MHz frequency range and its cross-sections from top (b) and bottom (c)

The 10 mm long tapered line (Fig. 2.1) improves the impedance matching from 50 Ω to 0.3 mm trace. The diameter of 0.4 mm was used to connect the top layer loop to the bottom ground layer polygon. SMA connector shield was soldered to copper pipe and PCB ground plane.

The improved probe has been compared with the standard same dimensions of planar near-field probe configuration. Two main field parameters have been modelled, i.e., field directly below the center of the probe and magnetic field strength with offset from the center axis. Three scanning distances of 3 mm, 5 mm, and 10 mm were chosen for the adaptive scanning height system. The model is presented in the Fig. 2.2.

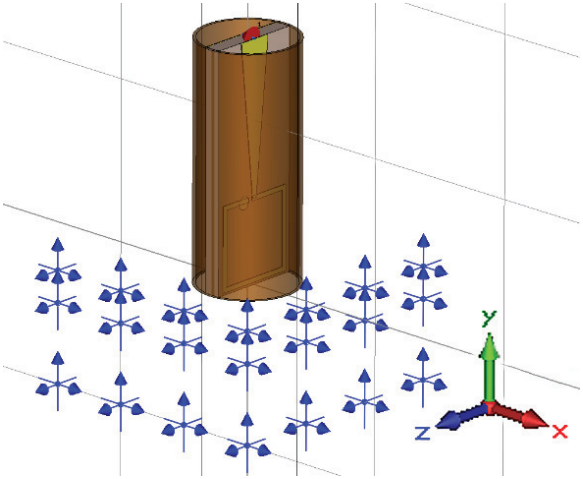

Fig. 2.2. Evaluation model of magnetic field focusing

For magnetic field suppression, the magnetic field strength at 5 mm, 10 mm, and 15 mm offset from the center spot was measured by adding wideband field measuring probes in CST Studio Suite environment. The simulation has been done for two axis, i.e., z and x, and the absolute values have been evaluated.

The simulation results for x and z axis are provided in the Fig. 2.3. The x axis comparison showed that the field directly under probe at 3 mm scanning distance increased from 0.5 dB to 3.1 dB, while 15 mm offset field suppression ranges from 10.1 dB to 12.1 dB; 5 mm scanning height case reveals suppression of 8.8–10.9 dB. However, at 15 mm scanning height, the field directly below probe has reduced by 3.9–5.5 dB, the improved probe structure remained; the field suppression at 15 mm distance from center varies from 4.9 dB to 7.1 dB.

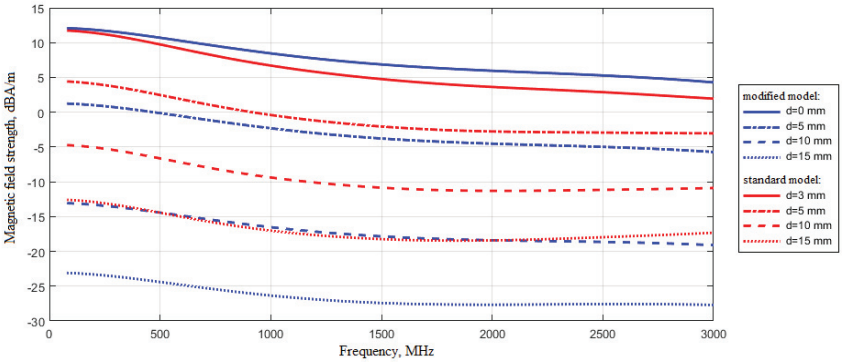

a

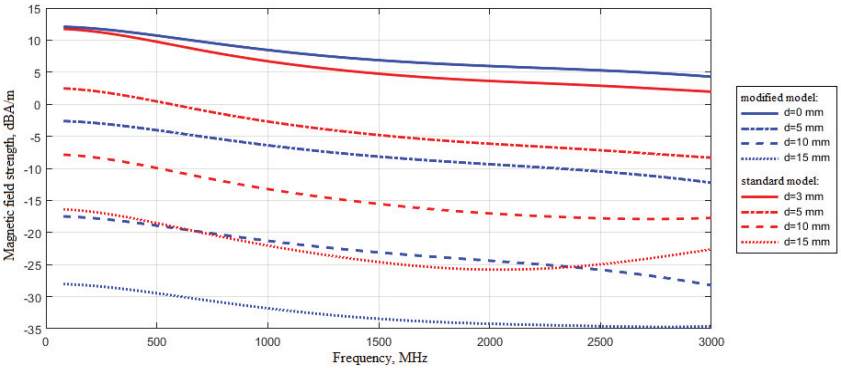

b

Fig. 2.3. Magnetic field intensity below improved and simple probes at 3 mm scanning height over 80–3000 MHz frequency range at x (a) and z (b) axis

The magnetic field analysis at z axis for 3 mm scanning height at 15 mm offset from the probe achieved suppression is in the range of 8.7 dB to 12.5 dB over the whole frequency range. At the increased scanning height of 5 mm, this field was suppressed by 8.2 dB to 12.2 dB. Finally, 10 mm scanning height shows magnetic field intensity reduction below the probe from 5.1 dB to 4 dB, but field suppression at 15 mm offset remains greater than 4.1 dB.

For coupling efficiency evaluation in RF susceptibility system, the mathematical model of improved magnetic near-field probe and 100 mm length receiving microstrip line has been developed in FEM software. The signal level at the microstrip line output was measured as a S_{21} parameter function from the scanning height h (Fig. 2.4).

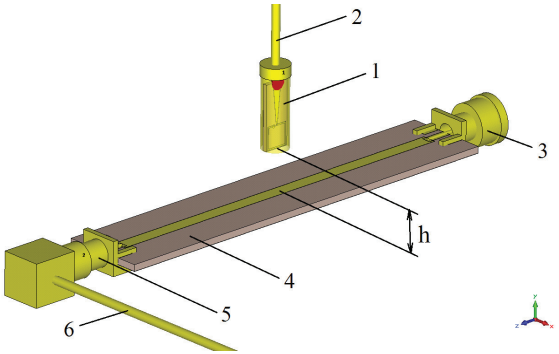

Fig. 2.4. Mathematical model of improved magnetic near-field probe and microstrip line for coupling efficiency evaluation in CST Studio Suite

The model structure is shown in the Fig. 2.4, where 1 – improved near-field magnetic probe, 2 – feed coaxial cable, 3 – matched 50 Ω load, 4 – PCB with microstrip line, 5 – microstrip line coaxial connector and 6 – cable for output.

5 simulations have been done for various h values: 3 mm, 5 mm, 10 mm, 15 mm, and 20 mm. The results of frequency range are provided in Figure 2.6.

For mathematical model verification, the setup has been designed and manufactured (Fig. 2.5). The jig consisted from 1) Keysight FieldFox N9916A portable microwave vector network analyzer (VNA) connected to 2) near-field magnetic probe, and 3) microstrip line is terminated with 4) 50 Ω matched load. The positioning of the probe and microstrip line and the height control are performed by 5) milled polycarbonate measurement jig.

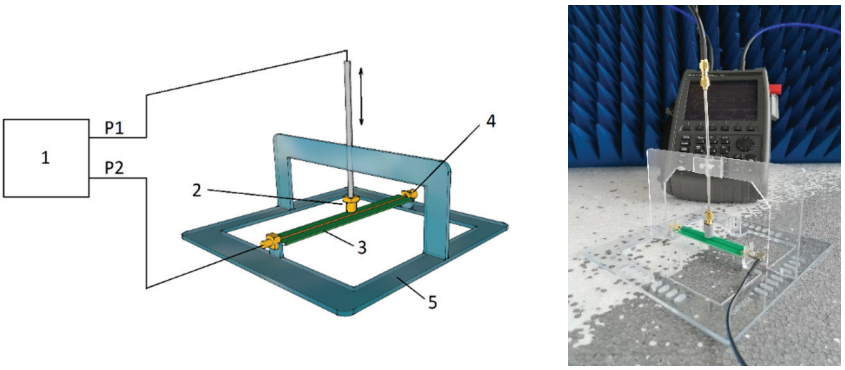

a b

Fig. 2.5. Mathematical model verification experiment structure (a) and the photo of the setup (b)

The comparison of modelling, measurement, and parasitic coupling results for mathematical model verification are provided in the Figure 2.6.

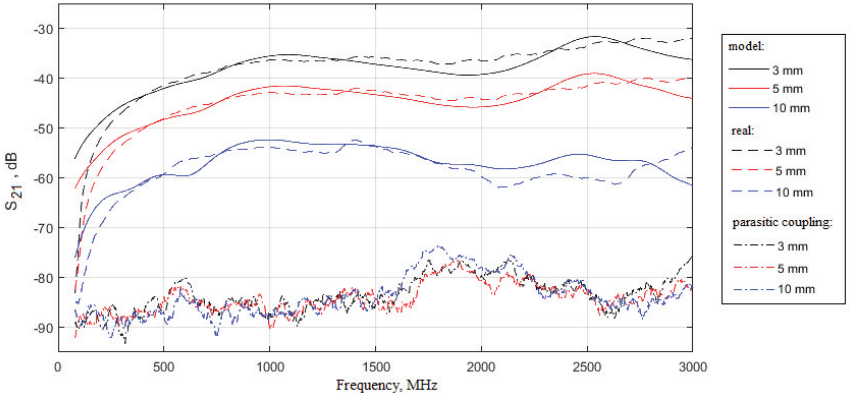

a

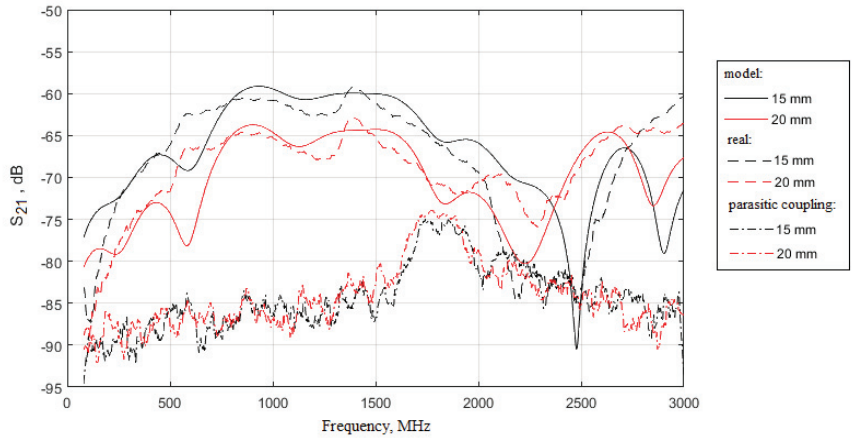

b

Fig. 2.6. Coupling efficiency results of the model and real setup overlaid by parasitic S_{21} for 3 mm, 5 mm, 10 mm (a), and 15 mm, 20 mm (b) scanning heights

The modelling results (Fig. 2.6) at the lowest frequency range starting from 80 MHz show the lowest coupling efficiency for 3 mm, 5 mm, 10 mm, and 20 mm; 15 mm scanning height trace has deep resonance at 2480 MHz. The modelling results provide useful information for the adaptive scanning height system for the compensation of coupling efficiency, as the scanning height changes through the scan. For VNA type scan, the output power could be set before the sweep; therefore, for setting system output power, the average

coupling efficiency was calculated over the whole frequency range and could be expressed as:

$$S_{21avg}(h) = 0.09406 \cdot h^2 - 4.094 \cdot h - 25.44, \quad (1)$$

where:

S_{21avg} – average value of coupling efficiency expressed by S_{21} parameter (dB), when the near-field probe is fed and signal level measured at the microstrip line output,

h – scanning height or distance between probe and microstrip line (mm).

For model verification, RMSE and percentage of samples fitting in the ±3 dB and ±6 dB range were calculated and listed in the Table 1.

Table 1. SMD resistor model parameters

Height, mm	**RMSE, dB**	**Percentage of frequency samples fitting in ±3 dB range, %**	**Percentage of frequency samples fitting in ±6 dB range, %**
3	9.21	91.00	97.60
5	8.12	92.70	97.60
10	9.56	71.53	95.50
15	14.94	61.44	76.92
20	11.66	72.42	85.21

The increasing of scanning height leads to higher differences between model and real measurement setup due to the lower coupling efficiency and more environmental influence. The analysis has shown greater than 76.92% of frequency samples results fitting inside ±6 dB range.

The magnetic field generated by near-field probe could be described in 3D vector shape; however, in order to analyze the field strength at scanning height, magnetic field cross-section should be analyzed as a projection on 2D plane. The shape of projection is similar to ellipse, which could be defined by two diameters, i.e., D_x and D_z (Fig. 2.7a). The limit is set to -6 dB of normalized field strength, which was introduced as -6 dB aperture.

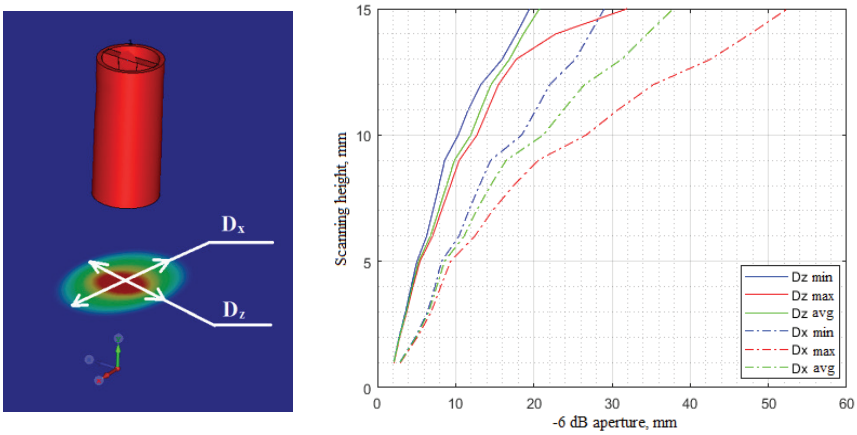

a b

Fig. 2.7. -6 dB magnetic field aperture - a and scanning height influence on it - b

The minimum, maximum, and average -6 dB magnetic field strength aperture diameters in x and z axis for various scanning heights are represented in Fig. 2.9b for 80–3000 MHz frequency range. The summarized results are presented in the Table 2 below.

Table 2. Standard deviation of near-field magnetic probe -6 dB aperture

	Standard deviation, mm			
	80–1000 MHz		**80–3000 MHz**	
Height, mm	**x axis**	**z axis**	**x axis**	**z axis**
1	0.0019	0.0041	0.0308	0.0109
3	0.0126	0.0111	0.1383	0.0538
5	0.0332	0.0190	0.3398	0.1288
10	0.2500	0.0748	2.4453	0.7148
15	0.8149	0.1465	7.5340	2.0862

The -6 dB aperture diameter standard deviation is below 2.4453 mm for scanning heights ≤10 mm for the full frequency range of 80–3000 MHz. The standard deviation of -6 dB aperture diameter is smaller for z axis, comparing to the x axis. For frequency range of 80–1000 MHz, the standard deviation is below 0.8149 mm for scanning heights of up to 15 mm.

3. DUT INFLUENCE ON RF SUSCEPTIBILITY MAPPING SYSTEM RESULTS

Commercial RF PCBs vary from simple single layer designs to multilayer hybrid high integration products containing IC and active components. Electronic components not only limit scanning height due to the physical dimensions but might introduce changes in electric and magnetic field strength around and below it.

The commercial product components' height analysis presents various heights of components starting from 0.35 mm for 0402 resistors up to 6.35 for voltage controllable oscillators (VCO) enclosed in BK377. Taking into consideration other RF connectors, adaptive scanning height limits for the optimization have been determined to be 1–15 mm.

Mainly two impedances, i.e., 50 Ω and 75 Ω, are dominant in RF PCBs; 75 Ω are often used in CATV (cable television) for lowering attenuation of long cables, while 50 Ω is mainly used in other RF equipment measurement systems, Wi-Fi, GSM, etc.

For the evaluation of impedance influence on near-field radiated susceptibility system, the modelling was done with magnetic near-field probe and two 10 cm length PCBs with matched 50 Ω and 75 Ω microstrip lines. The S_{21} parameter was used as coupling efficiency over the investigated 80–3000 MHz frequency range, and the difference plot between 50 Ω and 75 Ω impedances are represented in the figure below. The probe was actuated by 27 dBm power in the experiment and the loose end of PCB loaded by matched load.

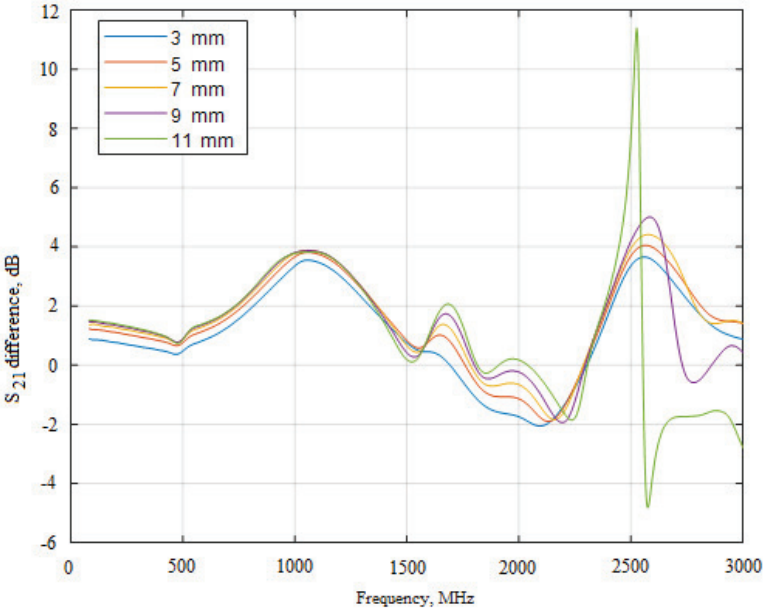

Fig. 3.1. Magnetic near-field probe and microstrip line coupling efficiency (expressed by S_{21} parameter) difference between 50 Ω and 75 Ω impedance cases over the frequency range of 80–3000 MHz for various scanning heights

The results presented in the Figure 3.1 reveal that the maximum S_{21} differences between 50 Ω and 75 Ω appear to be less than -2.1 dB to +5 dB for distances below 9 mm. In the case of 11 mm, the difference of frequencies above 2400 MHz significantly increases due to the resonance shift.

For the investigation of influence of various electronic components in the RF PCB on the magnetic field created by near-field probe SMD resistor, capacitor, the ferrite bead and RF balun finite element method (FEM) models have been developed.

The technical parameters for developed electronic component models were chosen according to Wurth, Panasonic, TDK, and Murata technical datasheets and specification notes.

Often, PCB layouts are aiming for high integration; therefore, commonly, 0402, 0603, and 0805 size components are used; 0805 size was chosen for the evaluation due to possibly the greatest influence on the field.

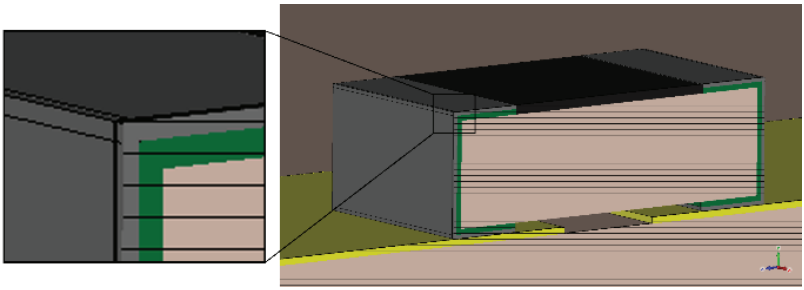

Fig. 3.2. 0805 SMD resistor in CST Studio Suit

1 kΩ nominal resistor model was designed on Al_2O_3 base with resistive carbon and protective glass layers. The SMT leads were formed from internal nickel (Ni) and external tin (Sn) layers (Fig. 3.2).

The multilayer ceramic capacitor (MLCC) based on X7R ceramic with 150 layer pairs was developed in CST Studio Suit. Due to the existing technology, SMT leads were constructed from internal connected to electrode pairs, middle and external tin contacts. A detailed capacitor model structure is provided in the Fig. 3.3.

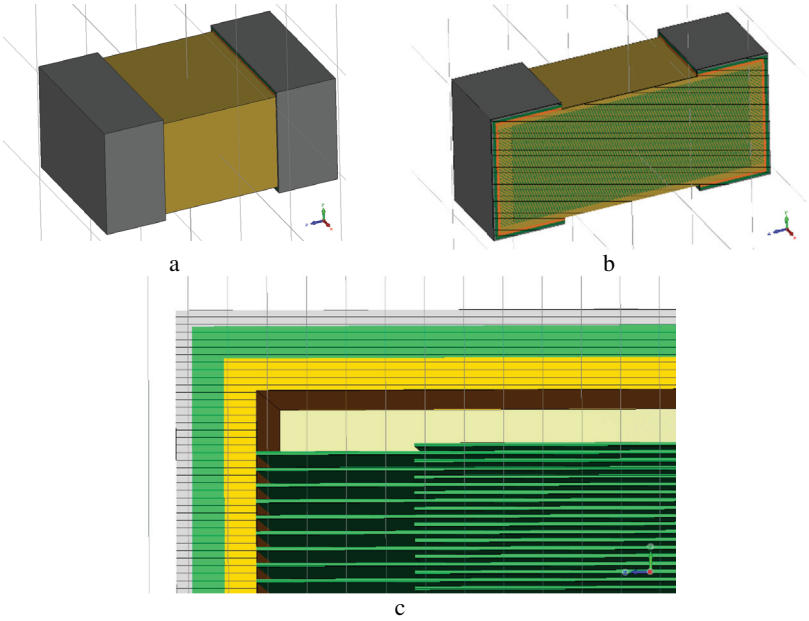

Fig. 3.3. 0805 SMD MLCC capacitor model (a) in CST Studio Suite, model cross-section (b), and zoomed fragment (c)

Finally, the inductive component model was developed using horizontal winding structure, often used for high frequency of RF designs. 16 spiral type windings are encapsulated in the NiZn ferrite block, connected through 3 layer contacts to form SMT leads. A detailed ferrite bead structure is provided in Figure 3.4 below.

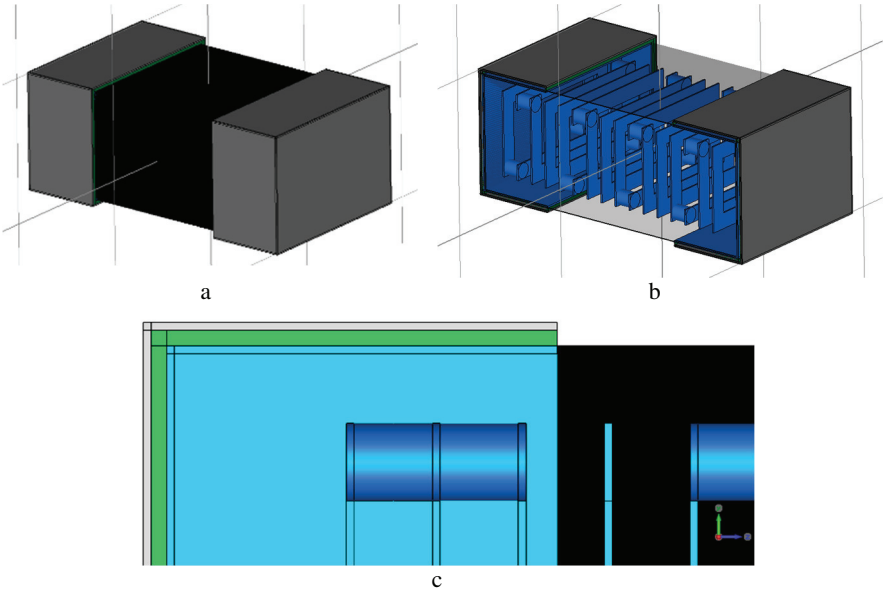

Fig. 3.4. 0805 SMD ferrite bead model (a) in CST Studio Suit, model with internal structure (b), and zoomed fragment of layers (c)

RF balun often used in push-pull or impedance transformation RF circuits is a very complex structure with a twisted pair of wires penetrating ferrite block. In the case of modelling, only base and ferrite was used due to the field attenuation and magnetic characteristics of ferrite material. MA-COM RF transformer MABA-007159-000000 was chosen for this research. The generalized balun structure is provided in Fig. 3.5.

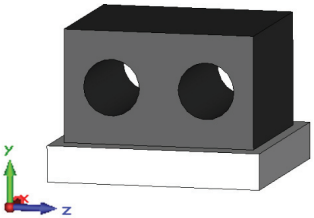

Fig. 3.5. 0805 SMD RF balun model in CST Studio Suit

Two types of evaluation experiments for the electronic components' influence on the magnetic field have been carried out in this research, firstly, the evaluation of magnetic field -6 dB aperture distortion in the open space environment. The modelling diagram is presented in Figure 3.6a below.

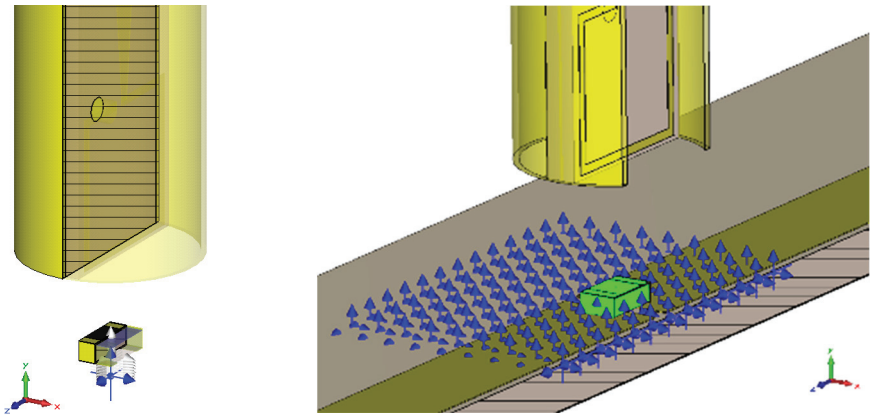

a b

Fig. 3.6. -6 dB aperture distortion evaluation (a) and magnetic field map distortion (b) modelling structure with transparent fragments to show probe orientation

Starting with -6 dB aperture distortion, the analysis has been done in the open space conditions; the magnetic field attenuation has been calculated for 8 points laid out by 0.1 mm step below component imitating 8 layers PCB with 0.1 mm layer separation. Two cases with generalized resistor component and greatest size balun were used in the research.

Feeding near field magnetic probe with 27 dBm, RF power at 3 mm distance from the component bottom, magnetic field attenuation over the frequency range 80–3000 MHz are provided below.

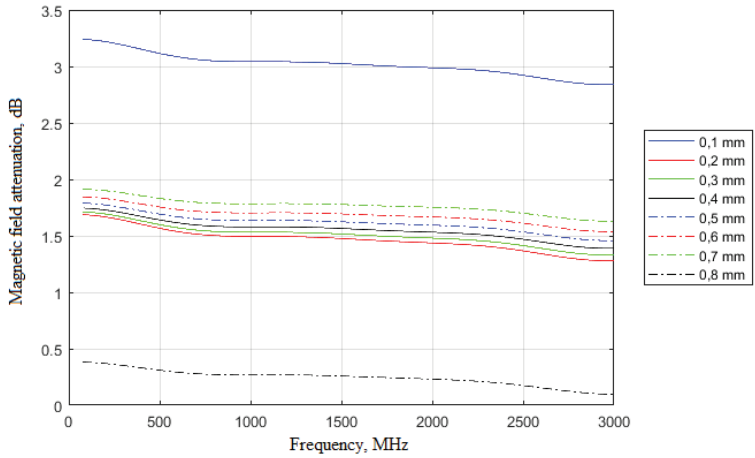

a

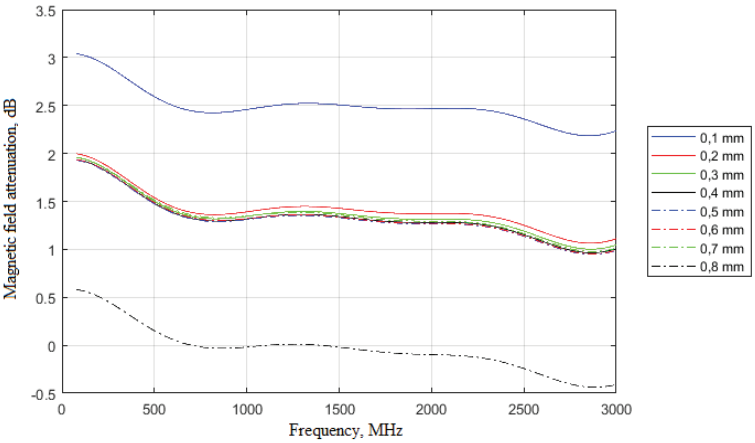

b

Fig. 3.7. Magnetic field attenuation due to the component presence in the near field magnetic type probe generated magnetic field depending on the distance below component for resistor (a) and RF balun (b)

In Figure 3.7a, the case of 0805 SMD resistor caused maximum magnetic field attenuation to be less than 3.25 dB, 0.1 mm below resistor. This attenuation is mainly caused by a relative magnetic permeability of nickel leads. The attenuation maximum was found at 80 MHz and the minimum at highest frequency range at 3000 MHz. At 0.8 mm distance below the resistor, the field attenuation was < 0.43 dB.

Magnetic field attenuation due to RF balun presented in Fig. 3.7b was noted to be below 3.1 dB at 0.1 mm below the balun base. For 0.2–0.7 mm distances, the results reduced to 1–2 dB; 0.8 mm distance, similarly to resistor case, has shown attenuation below 0.6 dB. Above 1500 MHz, the magnetic field increase up to 0.45 dB was registered.

For deeper analysis, the magnetic field distribution was evaluated taking into consideration PCB with microstrip line and the components assembled on it. For component persistence in the near-field probe generated magnetic field for 5 mm scanning height, 4 types of magnetic field distribution maps has been modelled: microstrip line without components and cuts, microstrip line with resistor, capacitor, and ferrite bead in the center of the line. All cases' magnetic field distribution maps, 0.1 mm below the signal conductor, are provided in Figure 3.8 below.

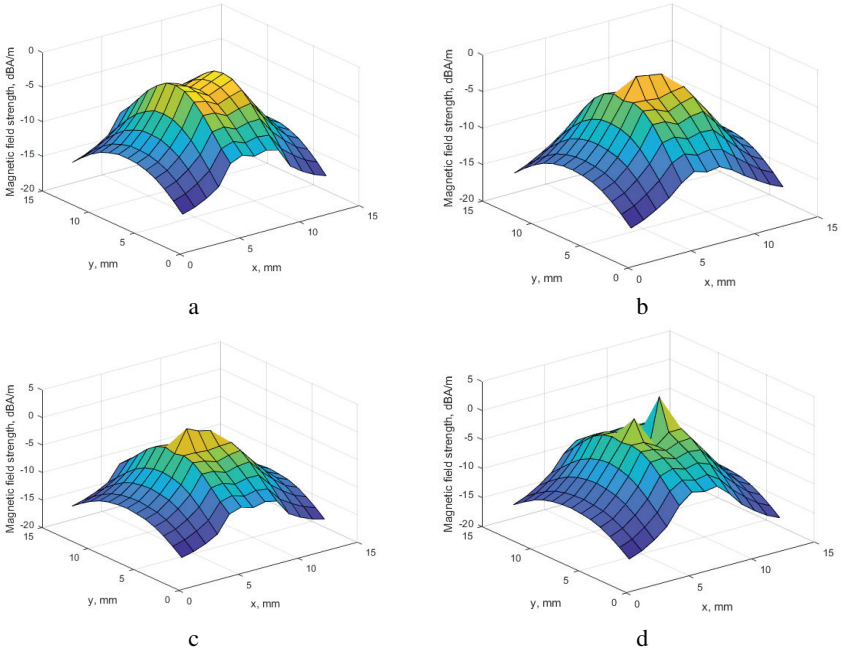

Fig. 3.8. Magnetic field distribution map 5 mm distance from the magnetic near-field probe in microstrip line (a) and microstrip line with resistor (b), MLCC capacitor (c) and ferrite bead (d) at 1000 MHz frequency

Though field distribution was simulated using 169 wideband magnetic probe array, typical 1000 MHz case is represented as result above. The valley in the center of the map was influenced by the signal conductor of microstrip line.

The ferrite bead case has spikes around the center caused by ferrite material. Resistor and capacitor maps showed similar results with increased intensity at the center of the map due to the cut in the microstrip line.

For more details, two cross-sections at XY and YZ planes are represented in the Figure 3.9 below. The field strength values were compared to the free space environment with measurement probes at the same distance from the near-field probe.

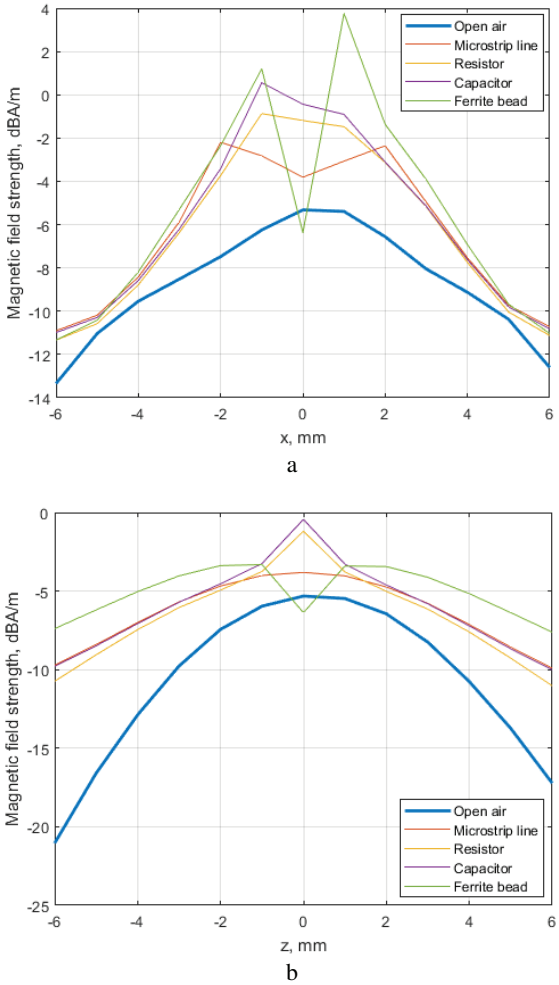

Fig. 3.9. Magnetic field distribution map cross-section at XY (a) and ZY (b) plane and 1000 MHz

The cross-sections at XY and ZY planes show increased magnetic field strength compared to the open air conditions. ZY cross-section provides flattering results due to the orientation of microstrip line trace. The absolute differences from open air for all the investigated cases have been calculated and provided in Table 3.

Table 3. Magnetic field distortion

Type	Max absolute difference from open air, dB					
	80 MHz		1000 MHz		3000 MHz	
	XY	ZY	XY	ZY	XY	ZY
Microstrip line	7.95	11.37	5.28	11.32	13.38	14.89
Resistor	8.90	13.49	5.38	10.30	2.40	11.84
Capacitor	8.65	11.46	6.81	11.25	9.86	16.58
Ferrite bead	12.22	15.92	9.15	13.65	10.46	13.71

The maximum absolute difference from the open air results have shown to be up to 16.58 dB difference for the capacitor ZY plane cross-section. The minimal difference was achieved with the resistor at the XY plane cross-section for 3000 MHz frequency.

All analyzed components have similar dimension nickel SMD leads. High difference variation up to 16.58 dB proofs that magnetic field distribution map is mainly influenced by the PCB layout and component electrical characteristics in the RF trace.

4. RADIATED RF SUSCEPTIBILITY MAPPING SYSTEM

For the radiated susceptibility maps of RF PCB, magnetic probe based near-field scanning system was designed, optimized, and analyzed for 80–3000 MHz frequency range. The block diagram is presented in Fig. 4.1.

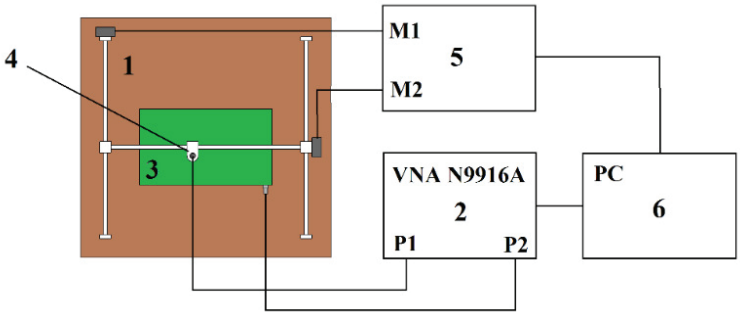

Fig. 4.1. Radiated RF susceptibility system diagram: 1 – x, y axis manipulator, 2 – VNA, 3 – DUT PCB, 4 – magnetic near-field probe, 5 – step motor driver, 6 – computer

For RF susceptibility mapping, PCB under test was fixed on non-conductive support. PCB output is connected to port 2 of VNA using coaxial cable, while any additional RF connectors are loaded with the matched load. The near-field probe input is connected to port 1 of VNA. Before scanning, probe height over PCB should be adjusted due to the protruding electronic components, and corrections should be set to ensure required magnetic field strength. Both x-y axis manipulator control and VNA triggering with data acquisition over 80–3000 MHz frequency range were done in PC by Matlab script. The physical realization of the developed system is presented in Fig. 4.2.

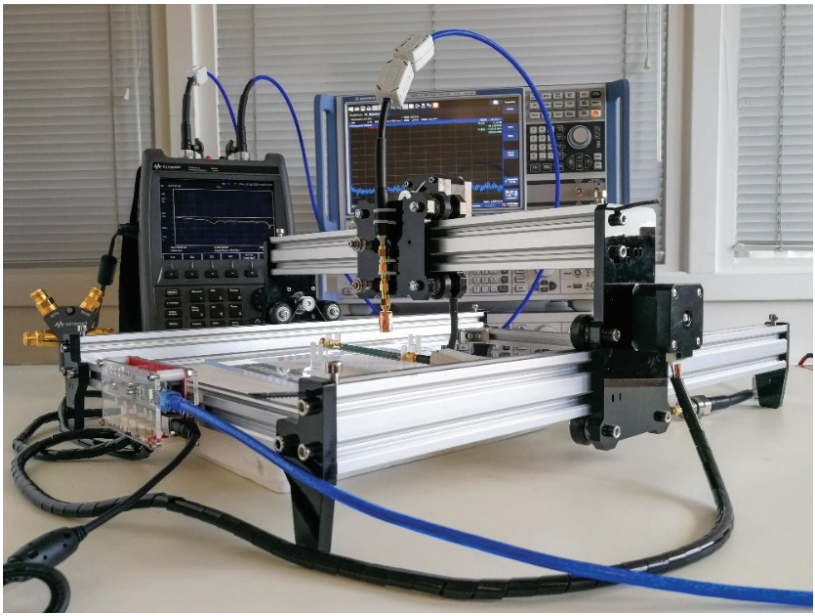

Fig. 4.2. Designed near-field radiated susceptibility mapping system

RF susceptibility maps are generated after the full scan of the PCB under test for each frequency sample individually, using S_{21} data recorded during the scan.

For designed system testing and verification, scanning was done with few simplified cases, where susceptible areas are easy to predict:

1. Microstrip line,
2. Coplanar line with RF gain block,
3. Coplanar line with RF amplifier and well-known problem in the PCB layout.

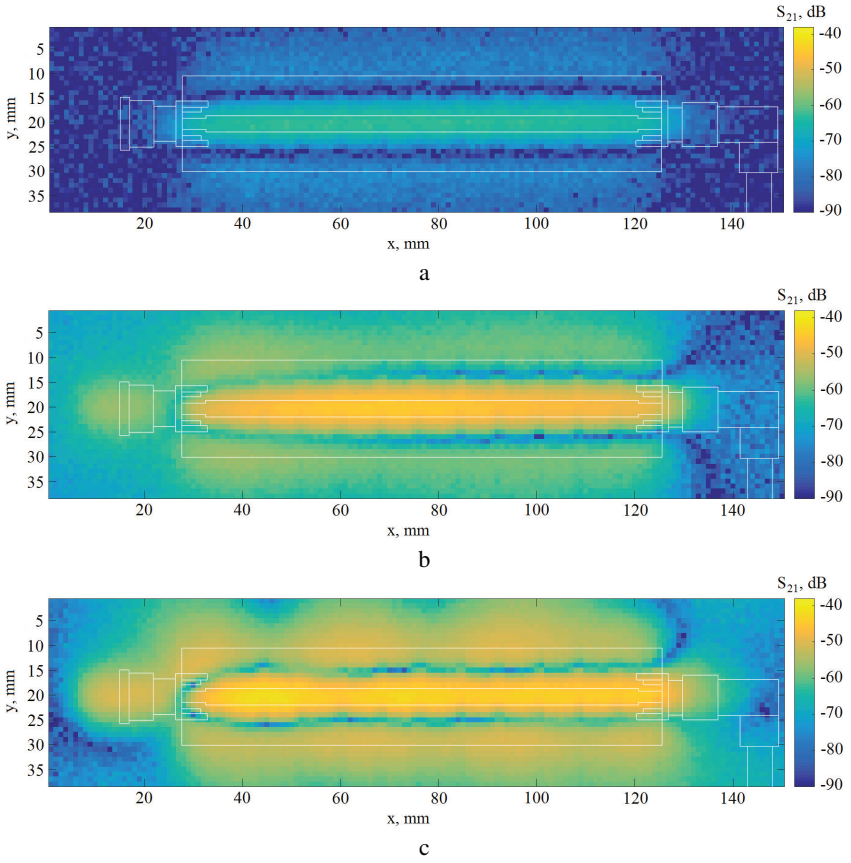

Fig. 4.3. RF susceptibility map of 10 cm length microstrip line PCB at 80 MHz - a, 1000 MHz - b, and 3000 MHz - c scanning frequency; PCB layout overlaid on the map

At the lowest frequency of 80 MHz RF susceptibility map (Fig. 4.3a), S_{21} parameter values are below -55 dB. Susceptibility hotspot region is located at the signal conductor of microstrip line. Ground polygon shows less sensitivity due to the bigger area and higher distance from the probe. 1000 MHz scanning frequency map presented in Fig. 4.3b shows increased sensitivity due to better coupling efficiency S_{21} reaching -44 dB. Highest sensitivity region is detected at the center of signal conductor, while 3000 MHz (Fig. 4.3c) shows more peaks and valleys over the signal conductor, due to the physical length of PCB versus wavelength.

The following analysis has been done with a more complicated PCB, having an active RF gain block ADL5536 at the center of coplanar line (Fig. 4.4).

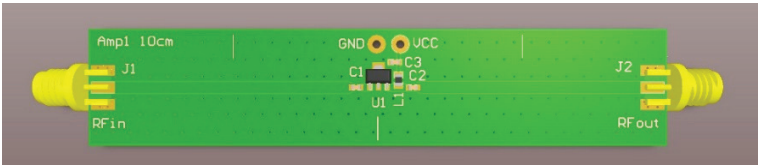

Fig. 4.4. PCB under test layout with coplanar line and RF gain block

S parameters of active RF PCB have shown S_{11} < -10.9 dB and S_{22} < -15 dB in the frequency range (Fig. 4.5) of designed operation < 1 GHz and gain >17.9 dB, while S_{21} at 3000 MHz is still 13.16 dB due to no filtering.

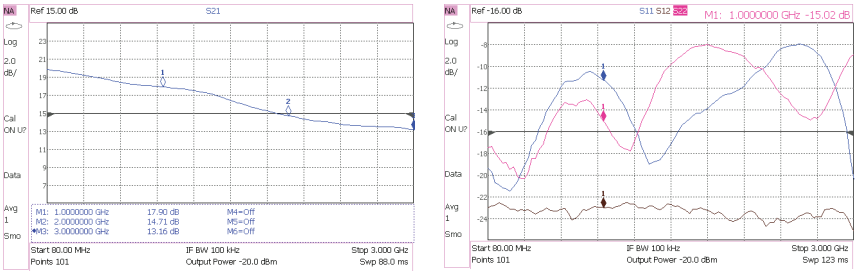

a b

Fig. 4.5. S parameters of the active RF PCB

The results (Fig. 4.6) present RF susceptibility map of the active RF PCB. From overlaid PCB layout, it could be clearly stated that the sensitivity at the amplifier input is higher due to the gain of the RF amplifier for a specific frequency. At 80 MHz, the sensitivity is the lowest due to relatively short size of the PCB for EM field wavelength. 1000 MHz frequency RF susceptibility map presents on average 15 dB greater sensitivity. Noticeable sensitivity appears at the output of the amplifier around the signal conductor of coplanar line and output SMA connector. 3000 MHz map analysis has shown the same hotspot location and up to 7 dB RF sensitivity increase at the input coplanar line signal conductor.

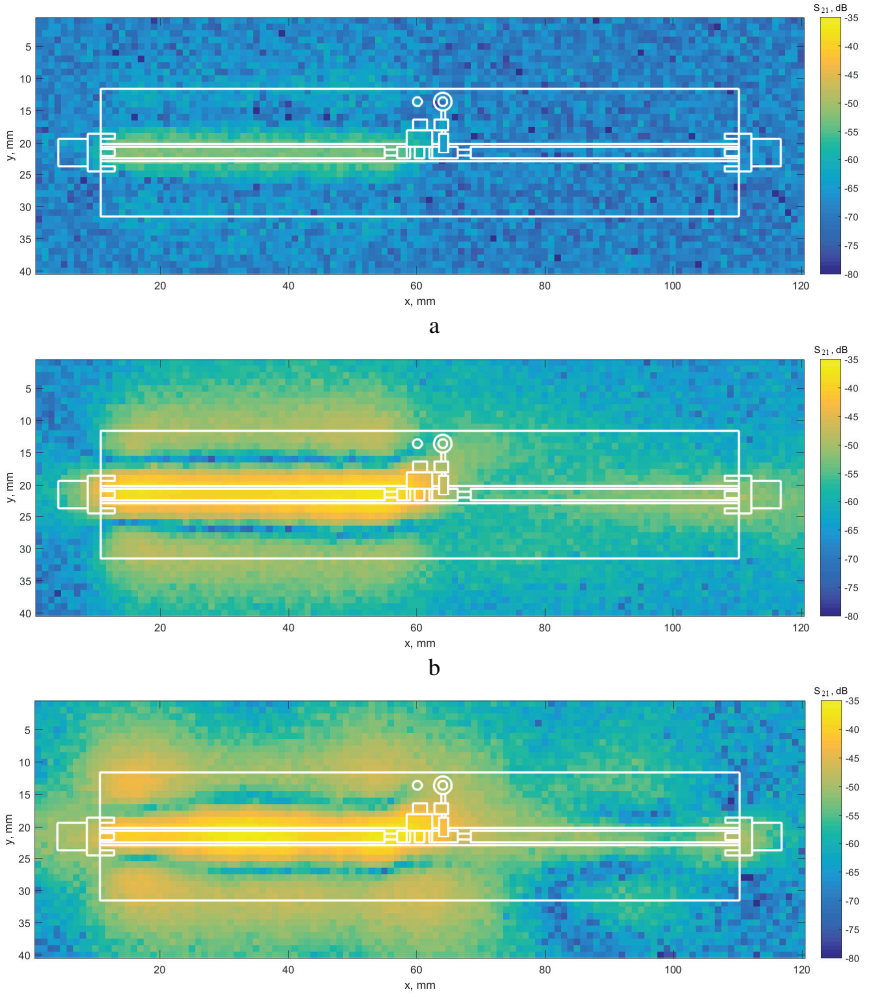

Fig. 4.6. RF susceptibility map of 10 cm length microstrip line PCB with gain block at 80 MHz - a, 1000 MHz - b, and 3000 MHz - c scanning frequency

For system ability to localize resonant type layout problems, active PCB is supplemented with 7 cm length open ended power track. This simplified case imitates the EMC problems of complex high integrity PCB, where single PCB exists for few assembly variants. Often, long power tracks connecting various PCB areas are left open ended without filtering capacitors. In this case, the designed PCB is presented in the Fig. 4.7.

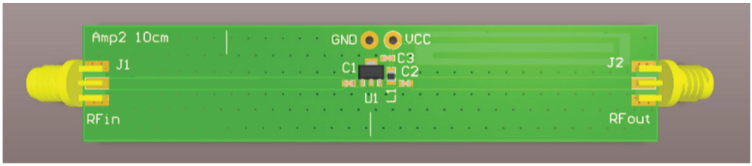

Fig. 4.7. PCB under test layout with RF gain block and open ended power track problem

The RF susceptibility mapping process was done in the full range, and the most typical cases with resonance and without are presented in the Fig. 4.8.

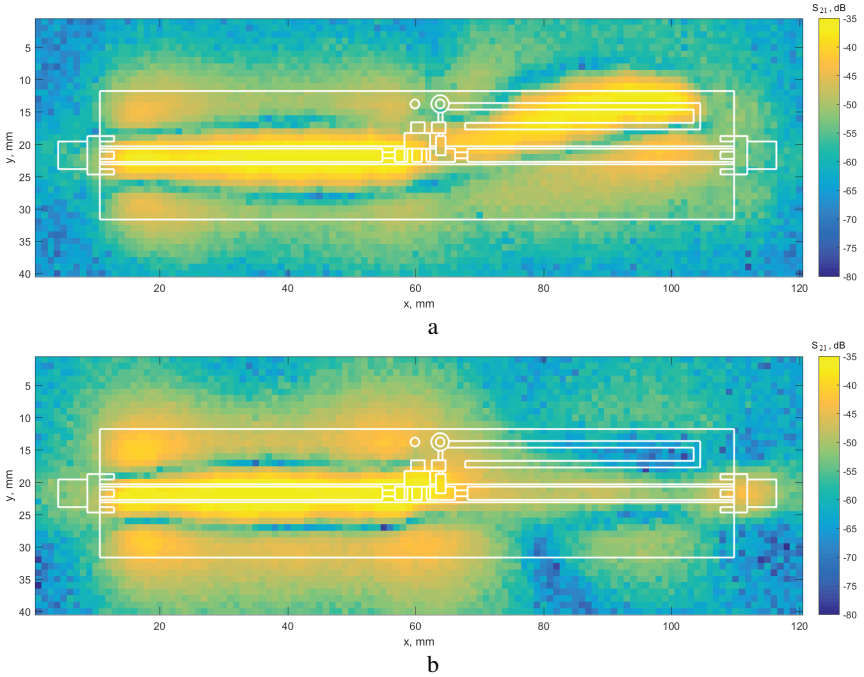

Fig. 4.8. RF susceptibility map of RF gain block PCB with open ended power track problem at 2130 MHz (a) and 3000 MHz (b) frequencies

As the results (Fig. 4.8) present, the system confirmed the ability to localize the problematic area, which influence was noticed over 1700–2600 MHz frequency range with maximum at 2130 MHz; 3000 MHz map case has shown only single hotspot at the input coplanar line.

In the previous experiments, the system has been tested with simplified cases. Commercial RF PCBs are high integrated and complex. For the purpose of

system verification on commercial RF products, the radiated susceptibility mapping has been done for 2 “Terra” cable TV RF products, starting with OR501W terrestrial TV fiber receiver module to high power broadband house amplifier HA210.

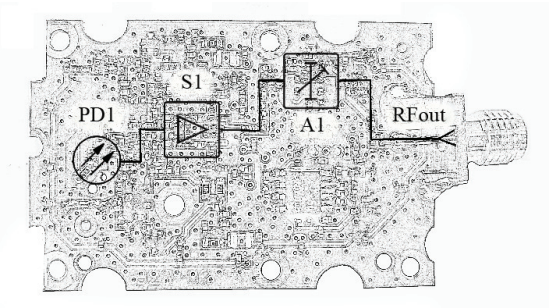

Fig. 4.9. Block diagram overlapped on the RF PCB layout of OR501W Terra fiber optics cable television (CATV) receiver module

The OR501W (Fig. 4.9) module is based on 1310 nm and 1550 nm photodiode PD1 with optical level control (OLC) feature. S1 RF amplifier works in transimpedance mode for matching photodiode impedance to 50 Ω and provides a signal gain. A1 voltage controllable PIN diode attenuator ensures a constant RF signal level in the OLC system.

As photodiode has been changed for 1 kΩ resistor, OLC system was set manually by external PSU (power supply unit). The RF susceptibility mapping has been done in 2 modes, i.e., at minimum and maximum A1 attenuation.

The results of OR501W CATV module susceptibility (Fig. 4.10) show lower RF susceptibility at 47 MHz compared to the higher operated frequency range limit. The maximum S_{21} value, due to small dimensions in both a and b cases, is below -67 dB. The minimum attenuation maps a and c shows hotspots at both PIN diode attenuator section and RF output connector. 862 MHz map shows up to 23 dB higher sensitivity compared to 47 MHz frequency.

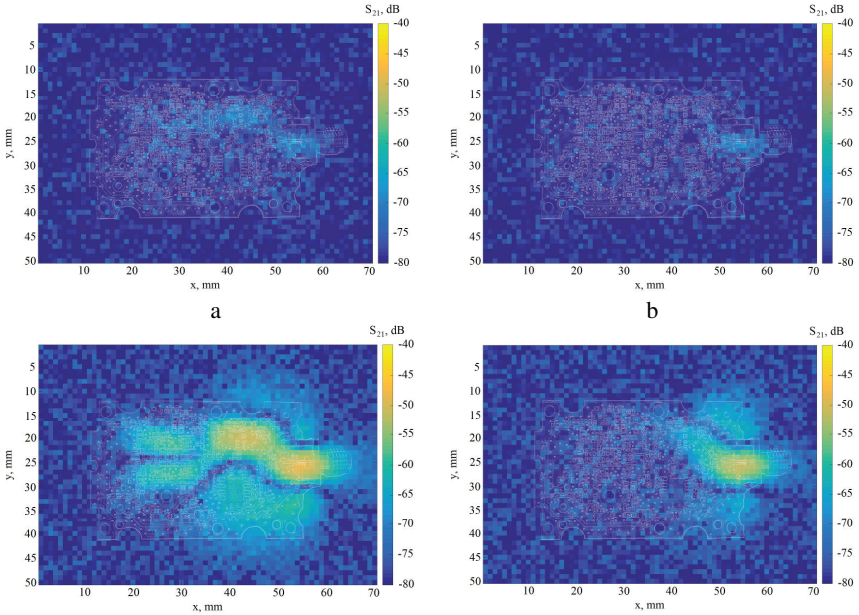

Fig. 4.10. Radiated susceptibility maps of Terra OR501W fiber optics CATV receiver module at operation frequency range; 47 MHz frequency with min (a) and max (b) attenuation and 862 MHz with min (c) and max (d) attenuation

From the frequency range, RF susceptibility maps (Fig. 4.11) show similar hotspot locations, which are more intense at RF output connector location due to the limited frequency response of the DUT amplifier.

The commercial product PCB RF susceptibility maps provide important information about the internal structure and RF components that might contribute to the RF susceptibility troubleshooting in the “Fail” scenario of EMC radiated immunity tests.

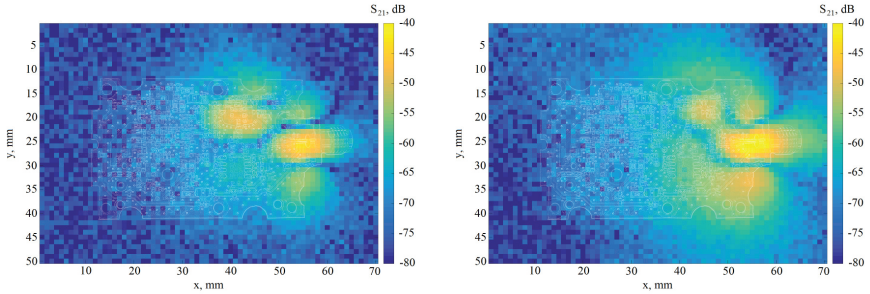

Fig. 4.11. Radiated susceptibility maps of Terra OR501W fiber optics CATV receiver module for out of band 3000 MHz frequency with PIN attenuator set to minimum (a) and maximum (b)

Finally, the verification has been carried out with 100 mm x 56 mm size board with complex multistage RF amplifier combined from the integrated circuit (IC) and discrete components as well attenuator and equalizer controls. Terra HA210 house amplifier was chosen due to the complex structure and a variety of components presented in Fig. 4.12.

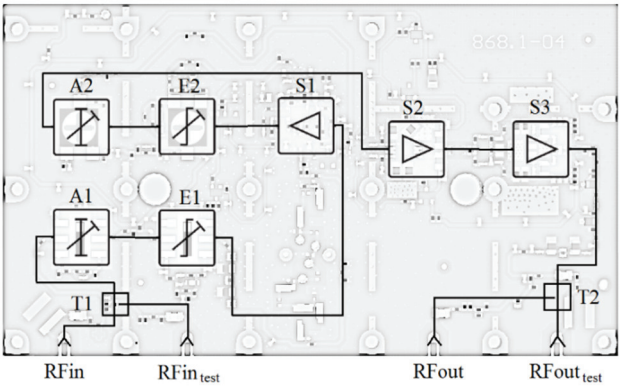

Fig. 4.12. Structure diagram of CATV house amplifier Terra HA210 overlaid on the amplifier PCB layout

The main structure consists of 3 stage RF amplifiers: S1, S2, and S3, input A1 and interstage A2 attenuators, and resistor based test points. The amplifier is equipped with E1 and E2 equalizers for input signal and interstage frequency response equalization. HA210 product complies with the EMC standards and is fully enclosed in the die cast aluminum enclosure. Because of the testing purpose and sensitive areas' localization, PCB has been scanned without enclosure.

The scanning height was set to 7 mm due to the presence of control potentiometers and other higher components such as gas dischargers at input and output. The amplifier frequency range starts at 47 MHz, but due to low sensitivity, only 450 MHz are displayed in the map (Fig. 4.13).

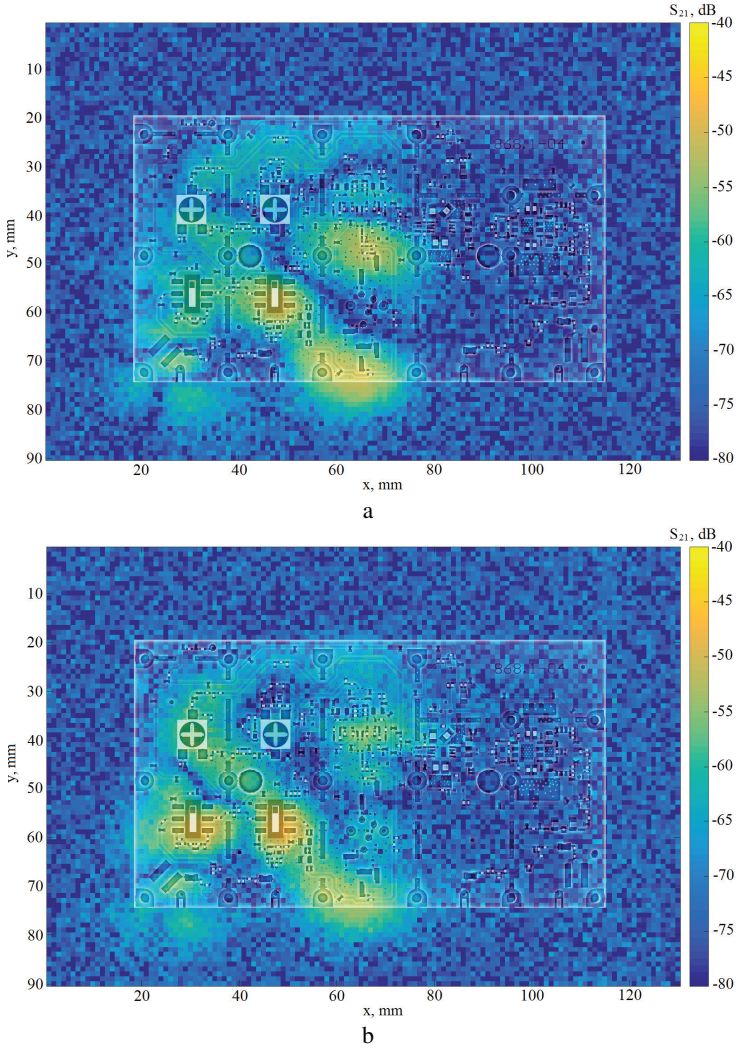

Fig. 4.13. RF susceptibility map superimposed with PCB layout of Terra HA210 at 450 MHz (a) and 1000 MHz (b)

At 450 MHz frequency (Fig. 4.13), the most sensitive areas are located at the input equalizers switch and RF tracks before the first amplifier. 1000 MHz RF susceptibility map presents similar locations, but the input attenuator and first push-pull amplifier susceptibility have increased. There were no significant hotspots at the output of RF PCB.

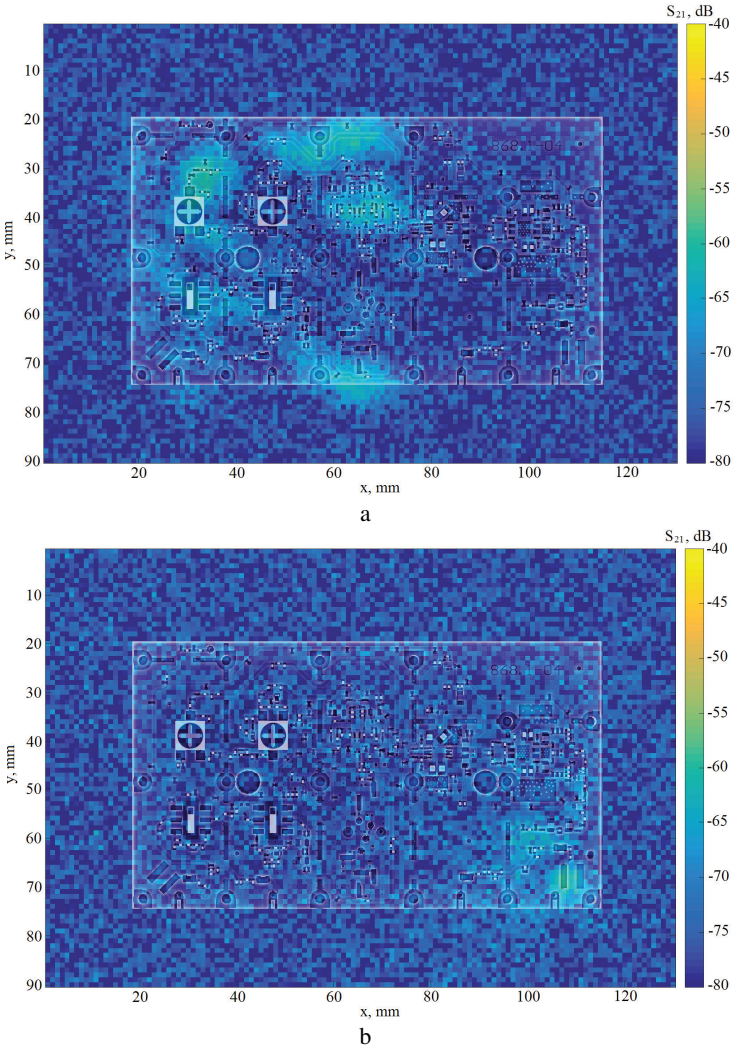

Fig. 4.14. RF susceptibility map superimposed with PCB layout of Terra HA210 from the operating frequency range at 1500 MHz (a) and 3000 MHz (b)

From the band RF susceptibility map (Fig. 4.14) of HA210, PCB shows less sensitivity on RF input tracks. At 1500 MHz, the amplifier interstage filtering was inefficient, thus showing sensitivity hotspots at controllable attenuator, RF input tracks and first active stage, while in 3000 MHz map, the sensitivity is noticeable at the output connector and RF output gas discharger. This frequency is effectively filtered in-between amplifiers stages.

The new method for radiated susceptibility pre-scan time minimization was developed by utilizing -6 dB magnetic field aperture size. As detailed maps might contain valuable information for high integrity PCB layouts, commercial PCB often has few dense sectors and other light integrated areas, where high resolution scanning has no advantages.

As a solution for reducing pre-scanning time, adaptive methodology has been developed. The scanning path and step sizes are presented in the Fig. 4.15 below.

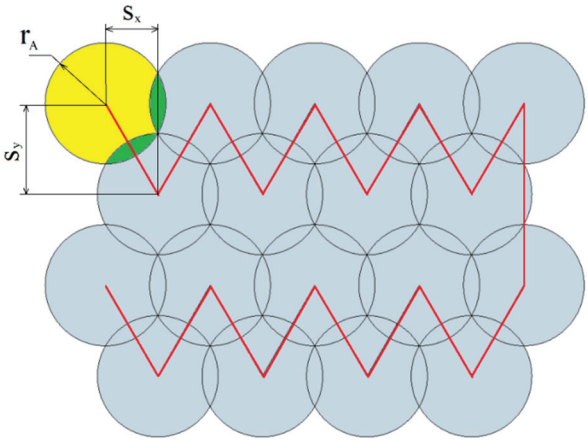

Fig. 4.15. Faster RF susceptibility pre-scan method based on -6 dB field aperture diameter

Pre-scan step sizes in x and y axis are calculated as follows:

$$s_x(h) = \frac{3 \cdot r_{ax}(h)}{2 \cdot \sqrt{3}}, \tag{2}$$

$$s_y(h) = 1.5 \cdot r_{ay}(h), \tag{3}$$

where:

$s_x(h)$ – scanning step size in x axis, $s_y(h)$ – scanning step size in y axis, h – scanning height above PCB board, $r_{ax}(h)$ – -6 dB aperture radius in x axis, $r_{ay}(h)$ – -6 dB aperture radius in y axis.

Though -6 dB aperture radius provides important details for step size calculation, it is lacking information on magnetic field distribution inside the aperture. Due to the physical dimensions and influence on the field of the physical magnetic field probes, the map has been modelled in CST Studio Suite. As modelling offers ideal isotropic probes, 13 x 13 magnetic field probe matrix has been populated below probe for wideband measurements (Fig. 4.16).

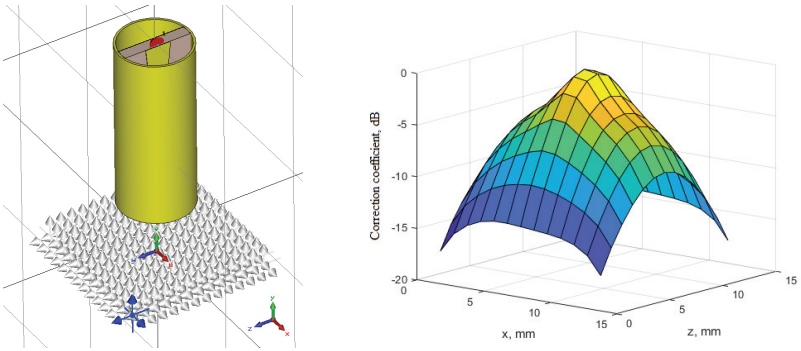

a b

Fig. 4.16. Model for improved near-field probe magnetic field distribution map measurement (a) and obtained normalized correction coefficient map (b) at 5 mm height and 1000 MHz

The magnetic field map 5 mm below probe was normalized and recorded as correction coefficients matrix provided in the figure above as a typical 1000 MHz case. All frequency maps could be separately used later in radiated susceptibility maps post-processing.

For the verification of proposed pre-scan method, RF susceptibility map of coplanar line size of 100 mm x 20 mm with active gain block was scanned over 120 mm x 40 mm area. Firstly, the measurements had been done, and for map post-processing probe correction, the coefficients were not evaluated. The whole area below probe is treated as the same sensitivity (Fig. 4.17a). In this case, due to similar sensitivity, higher intensity hotspot located with offset or lower intensity located at the center below probe provided similar results. The second map (Fig. 4.17b) is processed with probe correction map coefficients, evaluating the pattern of field strength below the probe. Both maps are presented in comparison to high resolution map (Fig. 4.17c).

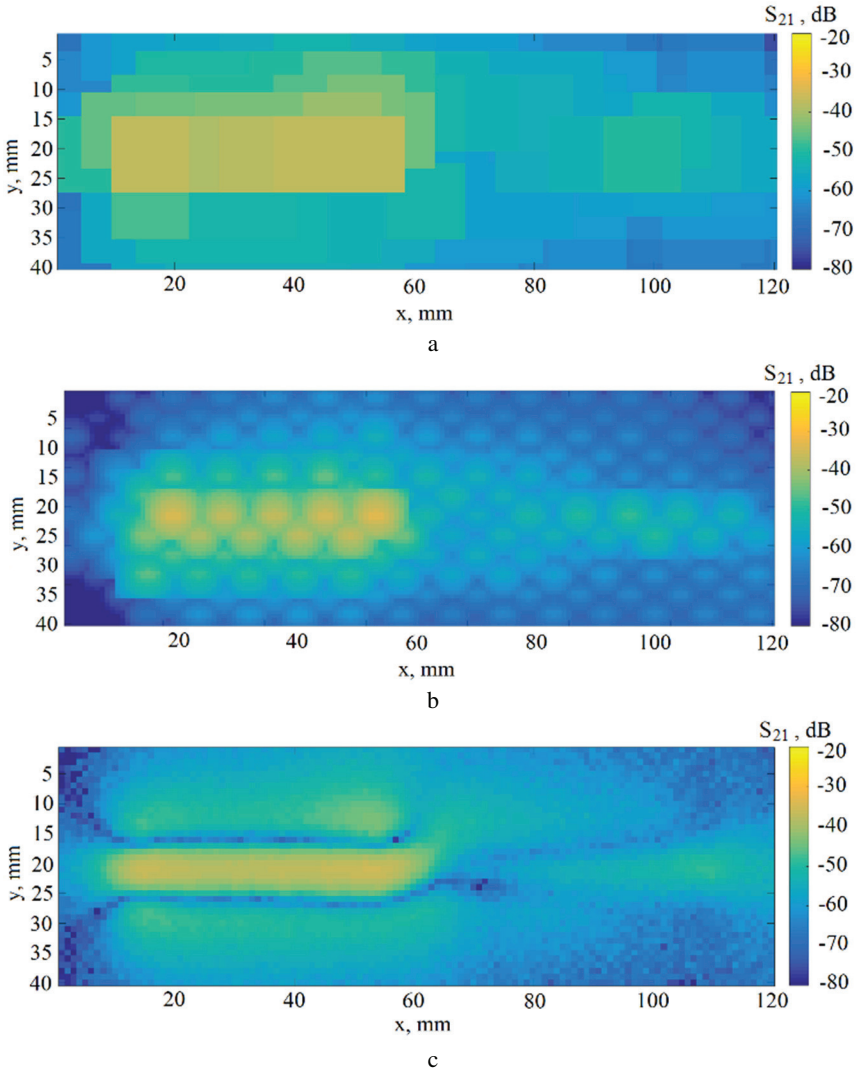

Fig. 4.17. RF susceptibility pre-scan map of coplanar line with active gain block at 5 mm scanning height and 1000 MHz with no correction coefficients (a), with correction coefficients (b) comparing with the high resolution scan (c)

Fig. 4.17 presents a hotspots area mainly on the left side of the map, where the input coplanar line of the gain block is located. Some intensity could be found at the output connector of the PCB.

To sum up, compared to the full high resolution scan maps, the hotspots location was correctly spotted.

For further improvement of the pre-scan method, additional high resolution rescan should be done at the detected higher RF susceptibility hotspots for improving localization precision.

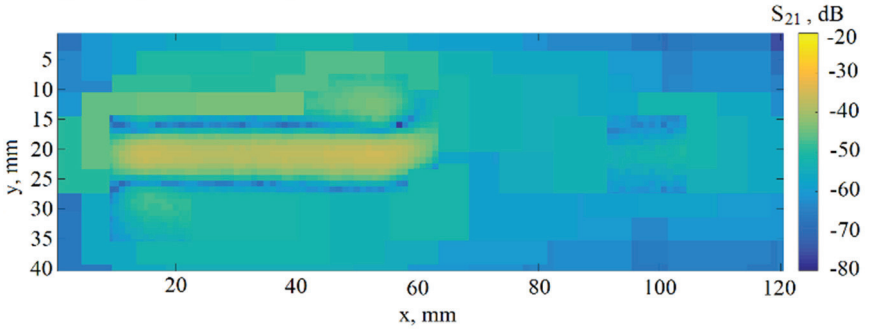

Fig. 4.18. Combined RF susceptibility pre-scan map of coplanar line with active gain block at 5 mm scanning height and 1000 MHz

Fig. 4.18 presents the combined pre-scan method result of RF susceptibility map, which was obtained firstly with lower resolution pre-scan for hotspots localization, later, corrected by full resolution scan only for localized higher intensity areas. This map provides valuable information for high integrated PCB areas and reduces the scanning time of irrelevant areas.

CONCLUSIONS

1. The analysis of radiated susceptibility testing methods shown insufficient approbation and characterization of near-field probes that provide guidelines for near-field improved spatial resolution magnetic field probe research and development.
2. New topology improved spatial resolution magnetic near-field probe characterization has shown that -6 dB magnetic field strength aperture dimensions fit within 12.9 x 26.3 mm for scanning heights up to 10 mm in free space and frequency range 80–3000 MHz.
3. The utilization of proposed probe aperture analysis and evaluated influence of PCB relief determined that pre-scan methodology allows minimizing the scanning time up to 64% for PCB sizes up to 100 mm x 100 mm.
4. The modelling of various SMD electronic components' influence on -6 dB magnetic field strength aperture determined that PCB layout and electronic component frequency response have the most significant effect on the magnetic field. The developed mathematical model of magnetic near-field

probe and microstrip line as PCB under test coupling efficiency was determined. Signal level variation from PCB dimensions has not exceeded 13.32 dB for 80–1000 MHz and 6.54 dB for 1000–3000 MHz.

5. The magnetic field vector analysis of proposed near-field probe has shown that the difference between orientations is significant and greater than 21.20 dB. This characteristic could be utilized for multi-orientation scanning algorithm development and provide useful information for high integrity electronics PCB RF susceptibility hotspot localization.
6. The localized radiated susceptibility hotspots of commercial cable television amplifier were confirmed by GTEM cell testing results received by changing operation modes (controlling the attenuator and equalizer in different locations).

REFERENCES

1. ETSI. TS 138 104 - V15.3.0. 5G; NR; Base Station (BS) radio transmission and reception (3GPP TS 38.104 version 15.3.0 Release 15). ETSI, 2018. [Online]. Available: https://www.etsi.org/deliver/etsi_ts/138100_138199/138104/15.03.00_60/ts_138104v150300p.pdf. Internet access: 2019-03-07
2. IEC. International Standard IEC 61000-4-3. Electromagnetic compatibility (EMC) – Part 4-3: Testing and measurement techniques – Radiated, radio-frequency, electromagnetic field immunity test. *IEC*, 2006.
3. IEC. International Standard IEC 61000-4-21. Electromagnetic compatibility (EMC) – Part 4-21: Testing and measurement techniques – Reverberation chamber test methods. *IEC*, 2011.
4. DAM, F. J. V. A Stripline antenna for radiated immunity. 2011. [Online]. Available: https://essay.utwente.nl/61201/1/Stripline-Frank-20111027_14u45-v0073-Final_PDF3.pdf. Internet access: 2018-02-09
5. WEN, L., YALIN, G. and JIN, L. Three new strip-line TEM cells in EMC test. *IEEE Int. Conf. Electron. Inf. Commun. Technol. ICEICT 2016*, pp. 497–500, 2016, doi: 10.1109/ICEICT.2016.7879750.
6. ISO. International Standard ISO 11452-4. Road vehicles — Component test methods for electrical disturbances from narrowband radiated electromagnetic energy - Part 4: Harness excitation methods. *ISO*, 2011.
7. VANHEE, F., GIELEN, G. & CATRYSSE, J. The use of BCI techniques regarding immunity testing of modules, as an alternative method up to 1 GHz. *EMC'09/Kyoto*. IEICE. 2009. pp. 685–688.
8. TIAN, Z., HUANG, Y., and XU, Q. Efficient measurement techniques on OTA test in reverberation chamber. *2017 IEEE Antennas Propag. Soc. Int. Symp. Proc., vol. 2017-Janua*, pp. 1855–1856, 2017, doi: 10.1109/APUSNCURSINRSM.2017.8072970.

9. MONTROSE, M. I., and NAKAUCHI, E. M. Testing for EMC Compliance. Approaches and Techniques. *Piscataway: A John Wiley & Sons*. 2004.
10. JOMAA, K., NDAGIJIMANA, F., JOMAAH, J., and AYAD, H. .Near-field measurement system with 3D magnetic-field probe design for dosimetric applications. *2016 IEEE Middle East Conference on Antennas and Propagation (MECAP),* Beirut, 2016, pp. 1-4, doi: 10.1109/MECAP.2016.7790103.

PUBLICATIONS

In editions refered on the databases from the Institute of Scientific Information (ISI):

1. MERFELDAS, A., P. KUZAS, D. GAILIUS, Z. NAKUTIS. Magnetic probe for improvement of near-field resolution in radiated susceptibility mapping. *Electron. Lett.*, vol. 55, no. 17, pp. 940–942, 2019.
2. MERFELDAS, A., P. KUZAS, D. GAILIUS, Z. NAKUTIS, M. KNYVA, A. VALINEVICIUS, D. ANDRIUKAITIS, M. ZILYS, D. NAVIKAS. An Improved Near-Field Magnetic Probe Radiation Profile Boundaries Assessment for Optimal Radiated Susceptibility Pre-Mapping. *Symmetry* 2020, 12, 1063.

In other rewieved scientific editions:

1. MERFELDAS, A., P. KUZAS, D. GAILIUS, and D. ANDRIUKAITIS, Characterization of radiated susceptibility directivity for microstrip and coplanar lines. *Proc. Eur. Microw. Conf. Cent. Eur. EuMCE 2019*, pp. 125–128, 2019.
2. MERFELDAS, A., P. KUZAS, D. GAILIUS, Z. NAKUTIS, M. KNYVA, A. VALINEVICIUS, D. ANDRIUKAITIS, M. ZILYS, D. NAVIKAS. Near-field Probe Radiation Profile Boundaries Assesment for Optimal Radiated RF Power Susceptibility Pre-maping. *13th international conference Elekto 2020*. Taormina, Italy, 2020., pp. 1-4.
3. MERFELDAS, A., D. ANDRIUKAITIS, D. GAILIUS, A. VALINEVICIUS, V. MARKEVICIUS, D. NAVIKAS, M. ZILYS. Field uniformity and TEM mode verification in GTEM 1000 cell. *13th international conference Elekto 2020.* Taormina, Italy, 2020., pp. 1-4.

Information about the author of the dissertation

Audrius Merfeldas was born on 11th of July 1986 in Kaunas, Lithuania.
In 2005, he graduated from VDU "Rasa" gymnasium.
In 2010, he obtained Bachelor of Electronics Engineering (study programme Electronics Engineering and Management) in the faculty of Telecommunications and Electronics at Kaunas University of Technology.
In 2013, he was awarded with Master of Science qualification degree of Electronics Engineering in the faculty of Telecommunications and Electronics at Kaunas University of Technology.
During 2016–2020, he studied in PhD study programme of Electric and Electronics Engineering, Department of Electronics Engineering at Kaunas University of Technology.
In 2016, he joined FABLAB Kaunas project as the Head of EMC laboratory at Kaunas University of Technology.

REZIUMĖ

Temos aktualumas

Šiuolaikinės elektronikos inžinerijos pasiekimais pagrįstų prietaisų ar sistemų projektavimo, testavimo, sertifikavimo etapai bei jų eksploatavimas realiomis sąlygomis yra artimai susiję su pašalinės elektromagnetinės (EM) spinduliuotės poveikio įvertinimu. Sparti bevielio ryšio paslaugų plėtra, daiktų interneto ir 5G įrenginių tankio ploto vienete didėjimas savo ruožtu kelia reikalavimus įrenginių elektroninės ir aukštadažnės dalies inžinerinių sprendimų kokybei. Naujų metodų, skirtų išsamiai įrenginio spausdintinio montažo plokštės analizei, pasiūlymas ir ištyrimas leistų ženkliai paspartinti schemotechninių sprendimų optimizavimą atsparumo EM trikdžiams požiūriu. Tai ypač svarbu medicininiams įrenginiams, automobilinei, karinės paskirties bei aviacijos elektronikai. Eksploatavimo metu prietaisas gali būti apspinduliuojamas iš artimoje aplinkoje ar maitinimo tinkle esančių pašalinės EM šaltinių. Taip pat prietaisas gali tapti normas viršijančios EM spinduliuotės šaltiniu dėl netinkamų inžinerinių ar konstrukcinių sprendimų. Standartais IEC 61000-6-1, IEC 61000-6-2 apibrėžiamos prietaiso atsparumo trikdžiams sąvokos, dažnių ruožai bei atsparumo lygiai gyvenamosioms ir industrinėms aplinkoms. Elektromagnetines emisijas bei jų leidžiamąsias ribas aprašo IEC 61000-6-3 ir IEC 61000-6-4 standartai.

Spinduliuojamų trikdžių emisijos ir atsparumas spinduliuojamiems EM trikdžių laukams reglamentuojami >80 MHz dažnių ruožui ir aktualūs visiems elektronikos gaminiams. Aukštutinė dažnių ruožo riba priklauso nuo produkto standartų bei testuojamų įrenginių rinkos segmento. Iš elektros tinklo maitinamiems prietaisams papildomai vertinami laidininkais sklindantys kondukuotų emisijų trikdžiai ir atsparumas jiems 150 kHz – 80 MHz dažnių ruože (IEC 61000-4-6). Šiems prietaisams taip pat keliami srovės harmonikų (IEC 61000-3-2, IEC 61000-3-12), mirgėjimo (IEC 61000-3-3, IEC 61000-3-11), atsparumo įtampos kryčiams, trūkiams (IEC 61000-4-11), viršįtampiams (IEC 61000-4-5), impulsų voroms (IEC 61000-4-4), srovės harmonikoms (IEC 61000-4-13) bei tinklo įtampos magnetiniam laukui (IEC 61000-4-8) reikalavimai. Siekiant užtikrinti kokybišką prietaisų veikimą ir atsparumą aplinkos poveikiams elektromagnetinio suderinamumo standartai reglamentuoja atsparumą elektrostatiniam išlydžiui, kuris tikrinamas visiems elektronikos gaminiams (IEC 61000-4-6).

Yra žinomos įvairios atsparumo spinduliuojamų trikdžių laukams testavimo metodikos. Pagrindinė ir labiausiai paplitusi – testavimas beaidžiame kambaryje. Šis principas pasižymi aukštu tikslumu ir atsikartojamumu, tačiau reikalauja itin didelių investicijų į laboratorijos įrangą: didelio galingumo aukštadažniai stiprintuvai, piramidiniais absorberiais ir ferito plytelėmis išklota

visiškai ekranuota patalpa bei galingos antenos, leidžiančios reikalaujamą lauką sukurti 10 m ar 3 m atstumais. Nors šios metodikos atsikartojamumas nenuginčijamas, testavimo rezultatų informatyvumas yra itin ribotas. Atlikus tyrimą gaunamas tik „Taip / Ne“ rezultatas skirtingiems trikdžių dažniams.

Pasauliniu lygmeniu dirbančių autorių moksliniuose darbuose aprašomi artimo lauko zondai tampa nepakeičiamu įrankiu, leidžiančiu lokaliai tyrinėti plokštę ir jos fragmentus, tačiau dauguma rinkoje esančių elektrinio ir magnetinio artimo lauko zondų ir su jais susijusių tyrimų yra skirti emisijoms. Artimo lauko zondų panaudojimas atsparumo spinduliuojamiems RF (radijo dažnių) trikdžiams tyrinėti nėra pakankamai ištirtas, todėl atsiveria mokslinių tyrimų niša. Taip pat susijusių mokslinių darbų analizė bei autoriaus asmeninė patirtis dirbant aukštadažnių elektronikos įrenginių projektavimo bei testavimo srityje rodo, kad rinkoje esantys zondai nėra optimizuoti atskiriems dažnių ruožams ir skirti tik preliminariai EM emisijų analizei. Be to, zondo sąveikos su testuojamu įrenginio fragmentu specifikacijos stoka gali komplikuoti probleminių plotų paiešką ypač didelės integracijos plokštėse ir paskatinti klaidingus EMC sprendimus, todėl atsiranda pagrįstas mokslinis ir inžinerinis poreikis bei motyvacija sukurti atsparumo spinduliuojamiems RF laukams tyrimo sistemą, paremtą artimo lauko zondu. Naudojantis šiuolaikinėmis EM laukų kompiuterinio modeliavimo priemonėmis, yra įmanoma zondo konstrukciją optimizuoti dažnių ruožui, spausdintinio montažo komponentų tipui, orientacijai ir kt. Autoriaus nuomone, šiuolaikinių didelės integracijos elektronikos įrenginių kokybiškai EM atsparumo specifikacijai tikslinga orientuotis į padidintos skyros PCB (spausdinto montažo plokštės) skenavimui skirto naujos topologijos zondo sintezę bei analizę, taip pat nuodugniai ištirti siūlomo zondo kuriamo lauko erdvinę struktūrą, sistemos parametrus ir elektronikos komponentų įtaką tyrimo rezultatams.

Darbo tikslas ir uždaviniai

Darbo tikslas – sukurti ir ištirti padidintos skyros artimo lauko skenavimo metodiką ir priemones elektroninės aukštadažnės įrangos atsparumo spinduliuojamų elektromagnetinių trikdžių poveikiui įvertinti.

Šiam tikslui pasiekti buvo iškelti **uždaviniai**:

1. Išanalizuoti ir palyginti elektroninės aparatūros atsparumo spinduliuojamiems elektromagnetiniams trikdžiams testavimo metodus.
2. Sukurti padidintos raiškos magnetinį artimo lauko zondą ir ištirti jo kuriamo magnetinio lauko stiprio dažnines, erdvines ir skyros charakteristikas 80–3000 MHz dažnių ruože.
3. Ištirti elektronikos komponentų artumo įtaką zondo kuriamo magnetinio lauko charakteristikoms.

4. Sukurti metodiką atsparumo spinduliuojamiems elektromagnetiniams trikdžiams skenavimo laiko minimizavimui.
5. Verifikuoti sukurtos metodikos efektyvumą elektromagnetiniams laukams jautrių aukštadažnių įtaisų spausdinto montažo plokštės vietų paieškai.

Mokslinis naujumas

1. Sukurta atsparumo spinduliuojamiems elektromagnetiniams trikdžiams artimo lauko skenavimo metodika, leidžianti sudaryti aukštadažnės įrangos spausdinto montažo plokštės jautrumo žemėlapius skirtingiems zondavimo dažniams bei lokalizuoti problemines vietas 80–3000 MHz dažnių ruože.
2. Pasiūlytas naujos topologijos padidintos skiriamosios gebos artimo magnetinio lauko zondas ir charakterizuoti jo kuriamo lauko parametrai.
3. Charakterizuoti spausdintinio montažo plokštės komponentų reljefo ir spausdintinio montažo plokščių takelių nulemiami pasiūlyto artimo magnetinio lauko zondo kuriamo lauko formos iškraipymai.
4. Sukurta pasiūlyto zondo apertūros ir plokštės reljefo įverčiais papildyta pirminio skenavimo metodika, leidžianti pagreitinti pirminį skenavimą vidutiniškai 31 %.

Tyrimų metodika

Prieš pasirenkant kuriamos sistemos konstrukciją bei parametrus buvo atlikta atsparumo spinduliuojamiems trikdžiams testavimo metodų analizė, išanalizuoti jų privalumai bei trūkumai. Nustačius, kad tik artimo lauko skenavimo metodas leidžia lokalizuoti jautrias PCB vietas, šis metodas pasirinktas sistemos realizacijai.

Išsikelti darbo uždaviniai reikalauja kompleksinių vektorinių ir daugiamačių elektromagnetinio lauko sprendinių, todėl jiems gauti buvo naudojami baigtinių elementų modeliavimo rezultatai, vėliau patikrinti eksperimentiškai.

Sukurto padidintos raiškos artimo lauko magnetinio zondo matematinio modelio sudarymui ir zondo optimizavimui buvo naudojama „CST Studio Suit“ modeliavimo programa, kurios rezultatai buvo apdirbti „Matlab“ programiniu paketu. Zondo kuriamas laukas vektorinis-erdvinis, be to, jo lauko stipris priklauso nuo dažnio, atstumo iki matuojamos plokštumos bei zondo galios. „CST Studio Suit“ programa buvo pasirinkta dėl patogių aukštadažnių parametrų išvedimo, optimizavimo galimybės.

Siekiant sukurti adaptyvaus skenavimo aukščio sistemą, atliktas magnetinio lauko stiprio ir injektuojamo signalo lygio priklausomybės vertinimas priklausomai nuo zondo aukščio virš PCB.

Siekiant įvertinti komponentų įtaką sukurti 4 elektronikos komponentų modeliai, kurių įtaka magnetinio lauko apertūros formos iškraipymams ir stiprio žemėlapiui įvertinta modeliuojant.

Sukurta sistema buvo patikrinta su supaprastintomis plokštėmis, kurių jautrios vietos lengvai prognozuojamos. Tolesnis sistemos testas atliktas su žinoma siaurajuoste PCB problema – rezonuojančio maitinimo takelio atšaka. Galiausiai sistemos analizė atlikta vertinant dviejų komercinių aukštadažnių gaminių PCB jautrumo spinduliuojamiems trikdžiams žemėlapius. Sistemos rezultatams palyginti su tolimo lauko sąlygomis atliktais testais, vienas komercinis gaminys papildomai įvertintas GTEM celėje.

Ginamieji teiginiai

1. Artimo lauko skenavimo metodika leidžia lokalizuoti EM trikdžiams jautrias aukštadažnių gaminių spausdinto montažo plokščių vietas, detalizuojant įrenginio problemines vietas.
2. Naujos konstrukcijos magnetinis artimo lauko zondas optimizuotas 80–3000 MHz dažnių ruože turi didesnį skiriamumo potencialą.
3. Naujas metodas paremtas -6 dB magnetinio lauko apertūra jautrumo spinduliuojamiems RF trikdžiams žemėlapių sudarymui sutrumpina skenavimo laiką.
4. Elektronikos paviršinio montažo komponentai įtakoja pasiūlyto artimo lauko zondo kuriamo magnetinio lauko -6 dB apertūrą.

Praktinė darbo vertė

Disertacijoje sukurtas atsparumo spinduliuojamiems trikdžiams artimo lauko skenavimo metodas gali būti pritaikytas pramonėje bei elektromagnetinio atsparumo tyrimų laboratorijose kompleksinių aukštadažnių spausdinto montažo plokščių (PCB) tyrimams. Skenavimo metu gauti elektromagnetinių laukų jautrumo žemėlapiai gali padėti tiksliau nustatyti aukštadažniams laukams jautrią plokštės vietą ir palengvinti elektromagnetinio suderinamumo problemų sprendimą.

Išvados

1. Išanalizavus elektroninės aparatūros atsparumo spinduliuojamiems EM trikdžiams testavimo metodus buvo nustatytas nepakankamas artimojo lauko magnetinių zondų pritaikomumo atsparumo testams aprobavimas ir charakterizavimas bei suformuluoti į padidintos skyros artimo magnetinio lauko zondavimą orientuoti moksliniai tyrimai.

2. Ištyrus sukurto naujos topologijos padidintos skiriamosios gebos artimo lauko magnetinio zondo charakteristikas, parodyta, kad zondo kuriamo artimo lauko -6 dB apertūros matmenys atviros erdvės sąlygomis 80–3000 MHz neviršija 12,9 x 26,3 mm skenavimo aukščiams iki 10 mm.
3. Ištyrus sukurtos pasiūlyto zondo apertūros ir plokštės reljefo įverčiais papildytos pirminio skenavimo metodikos veiksmingumą, nustatyta, kad pirminis iki 100 mm x 100 mm PCB skenavimas gali būti paspartintas iki 64 %.
4. Matematinio modeliavimo būdu įvertinus SMD elektronikos komponentų įtaką pasiūlyto zondo kuriamo magnetinio lauko stiprio ir -6 dB apertūros formai, nustatyta, jog didžiausią įtaką magnetiniam laukui turi PCB takeliai ir komponentų dažninės charakteristikos savybės. Panaudojus matematinius sukurto artimo lauko magnetinio zondo ir mikrojuostelinės linijos modelius įvertinta testuojamos PCB gabaritų įtaka injektuoto signalo lygiui. Signalo lygio variacija priklausomai nuo plokštės gabaritų neviršijo 13,32 dB 80–1000 MHz ir 6,54 dB 1000–3000 MHz dažnių ruožuose.
5. Ištyrus pasiūlyto artimo lauko zondo kuriamo magnetinio lauko vektorių orientaciją dažnių ruože, nustatyta, kad zondo kuriamo lauko stiprio skirtumas ortogonaliomis kryptimis yra ne mažesnis nei 21,20 dB. Ši zondo savybė, išnaudota skenavimo skirtingomis orientacijomis algoritmui sukurti, ir suteikia papildomą informaciją problemiškų PCB takelių ar komponentų orientacijai nustatyti didelės integracijos plokštėse.
6. Sukurtos artimo lauko atsparumo spinduliuojamiems trikdžiams skenavimo sistemos žemėlapiuose aptiktos jautrumo vietos skirtingų dažnių atvejais sutapo su GTEM celėje analizuoto komercinio aukštadažnio stiprintuvo jautriomis RF trakto vietomis, gautomis keičiant skirtingus režimus (įvedant ateniuatorių ir ekvalaizerį skirtingose vietose).

Trumpa informacija apie autorių

Audrius Merfeldas gimė 1986 07 11 Kaune.
2005 m. baigė VDU „Rasos“ gimnaziją.
2010 m. Kauno technologijos universiteto telekomunikacijų ir elektronikos fakultete įgijo elektronikos inžinerijos bakalauro laipsnį, baigęs elektronikos inžinerijos ir vadybos studijų programą.
2013 m. Kauno technologijos universiteto telekomunikacijų ir elektronikos fakultete įgijo elektronikos inžinerijos magistro laipsnį.
2016–2020 m. doktorantūros studijos Kauno technologijos universiteto elektros ir elektronikos fakultete, Elektronikos inžinerijos katedroje.
2016 m. prisijungė prie „FABLAB Kaunas“ projekto ir vadovauja elektromagnetinio suderinamumo laboratorijai.

UDK 621.391.82(043.3)

SL344. 2021-04-08, 3,25 leidyb. apsk. l. Tiražas 50 egz. Užsakymas 82.
Išleido Kauno technologijos universitetas, K. Donelaičio g. 73, 44249 Kaunas
Spausdino leidyklos „Technologija“ spaustuvė, Studentų g. 54, 51424 Kaunas